POLITECNICO
MILANO 1863

SCHOOL OF CIVIL, ENVIRONMENTAL AND LAND MANAGEMENT ENGINEERING
MASTER OF ENVIRONMENTAL AND LAND PLANNING ENGINEERING

REGIONAL MODELLING OF SEDIMENT CONNECTIVITY IN GRAVEL-BED RIVER NETWORKS

MODELLING FRAMEWORK AND APPLICATION TO THE UPPER PO BASIN

Master Thesis by:
Giulio Camisani
Student Id n.817025

Advisor:
Prof. Andrea Castelletti

Co-Advisor:
Dr. Simone Bizzi, Rafael Schmitt

Academic Year 2015 – 2016

Acknowledgments

I would like to thank prof. Andrea Castelletti, who gave me the opportunity to work on this thesis project and to address an interesting domain new to me.

Thanks to Rafael Schmitt, who introduced to me his "terrific creature" and helped me to deal with it.

I would like to thank Simone Bizzi for the great help and the time that he dedicated to my thesis.

I'm also grateful to the whole research group on natural resource management of the DEIB, and in particular to Enrico Weber, for technical assistance and advices.

Last, but not least, I would like to thank my family, my friends and whoever supported me (in every sense of the word) during the works for this thesis.

Abstract

Sediment connectivity is an important aspect to be considered in water resources management, which, however, implies modelling challenges at large scale, often preventing it from being properly implemented. A recent attempt to tackle this problem is represented by CASCADE model. CASCADE (**CA**tchment **S**ediment **C**onnectivity**A**nd **DE**livery) is a newly developed modelling framework (*Schmitt et al.*, 2016) combining concepts of graph-theory and sediment transport models. The approach describes the delivery of sediment mixtures originating from multiple sources in a river network by implementing individual transport processes, called "cascades". This allows to provide disaggregated information about provenance and destination of single sediment loads and so to quantitatively describe sediment connectivity in river networks, also for wide basins thanks to relatively little computational efforts required.

The main aim of this thesis is verifying the performances of CASCADE simulation on the network scale through the comparison with distributed sediment observations, with a particular focus on methodology and tools. This thesis focuses on the Upper Po river basin, for which more accurate data are available for both the calibration and the validation compared to the previous model applications. Moreover, as the Po River is basically characterised by gravel bed, it provides a novelty also from this point of view, since most previous CASCADE implementations focused on sandy rivers.

Before presenting the study site application, a detailed formalisation of the CASCADE framework is provided, introducing key aspects about conceptualisation of processes and MATLAB implementation necessary to carry out the simulation and the elaboration of final outputs. Secondly, the modelling framework is integrated with further components specially developed during this thesis work to exploit currently available high resolution topographic and multi-spectral data, used to model the river network under study. Specifically an automatic tool to extract the graph of the river network was implemented in MATLAB based on a digital elevation model and on the Topotoolbox functions by *Schwanghart and Kuhn* (2010).

The results of the simulation of sediment fluxes over the river network confirm the goodness of CASCADE model as a screening tool for large scale assessment of sediment connectivity, having provided qualitatively reasonable outputs and estimates quantitatively consistent with observed validation data. Specifically, large scale pat-

terns of bed material composition and total sediment flux agree with our conceptual understanding. Beyond, and this is the major finding of this thesis, CASCADE was able to reasonably represent observations of grain size and sediment flux data locally available for the river network under study.

Riassunto

La modellizzazione del trasporto solido fluviale su larga scala presenta delle difficoltà modellistiche che spesso ne hanno limitato l'applicazione nell'ambito della pianificazione e gestione delle risorse idriche, pur costituendo un importante aspetto da implementare per non incorrere in problemi di alterazione della morfologia fluviale. Il modello CASCADE rappresenta un recente esperimento in questa direzione. CASCADE (**CA**tchment **S**ediment **C**onnectivity**A**nd **DE**livery, *Schmitt et al.* (2016)) costituisce un nuovo approccio modellistico che introduce degli elementi di teoria dei grafi per la modellizzazione del trasporto solido in una rete idrografica. Rispetto ai modelli di trasporto solido precedentemente sviluppati, CASCADE consente di modellizzare i flussi di sedimenti conservando informazioni disaggregate su provenienza e destinazione di ogni singolo carico di sedimenti, rappresentando dunque uno strumento utile per esplorare la connettività del trasporto di sedimenti su larga scala. I costi computazionali contenuti consentono la simulazione anche per bacini idrografici molto estesi.

In questa tesi ci si propone di eseguire una simulazione dei flussi di sedimenti sulla rete fluviale del Piemonte, coincidente con la parte più a monte del bacino del Po, da validare con dati spazialmente distribuiti, e al contempo fornire una dettagliata descrizione dei processi modellizzati dal modello CASCADE e della loro implementazione in codice MATLAB.

Il caso di studio della rete idrografica dell'alto Po presenta delle interessanti novità rispetto alle precedenti applicazioni di CASCADE, in quanto svolto per la prima volta su un bacino per cui sono disponibili dati di alta qualità sia per la taratura che per la validazione del modello. Si tratta inoltre di una rete fluviale caratterizzata da sedimenti ghiaiosi, che costituisce quindi un test nuovo anche sotto questo punto di vista, essendo prevalentemente sabbiosi i sedimenti trasportati dai fiumi oggetto delle analisi precedenti a questo lavoro.

Prima di affrontare il caso di studio viene fornita una descrizione del modello CASCADE con particolare attenzione alla implementazione in codice MATLAB dei vari componenti, in cui vengono presentate le nozioni necessarie ad eseguire una simulazione e ad elaborarne i risultati. In secondo luogo viene descritta la procedura di pretrattamento dei dati, che ha previsto l'elaborazione di un nuovo componente, basato sulle funzioni del Topotoolbox di *Schwanghart and Kuhn* (2010), per l'estrazione della rete

fluviale a partire da un modello digitale del terreno ad alta risoluzione, nonché l'integrazione di dati di origine multispettrale necessari per la caratterizzazione morfologica della rete idrografica in esame.

I risultati della simulazione dei flussi di sedimenti nella rete fluviale confermano la validità del modello CASCADE come strumento di indagine per la valutazione della connettività dei sedimenti su larga scala. I risultati sono infatti qualitativamente ragionevoli e quantitativamente compatibili con i dati di validazione. Nel dettaglio l'andamento sulla rete fluviale dei flussi di sedimenti e della loro composizione granulometrica è coerente con le possibili considerazioni a livello concettuale. Inoltre, aspetto più interessante tra i risultati di questa tesi, con il modello CASCADE è stato possibile riprodurre in maniera soddisfacente i dati di validazione riguardanti la granulometria e i flussi di sedimenti localmente disponibili per la rete fluviale in esame.

Contents

List of Figures

List of Tables

CHAPTER 1

Introduction

Sediment connectivity, defined by *Bracken et al.* (2014) as the description of sediment transfer processes from sediment sources to sinks in terms of magnitude, transport time, and delivered grain size, is a relevant issue concerning water resources management, yet, so far, sediment connectivity has rarely been considered in operational water studies because it implies some major modelling challenges (*Schmitt*, 2016). Computational time and lack of wide-spread data have so far limited connectivity analyses to small and well monitored basins. Hence the necessity to develop a new model suitable for the analysis of all aspects of connectivity also at the scale of major river basins, such as CASCADE (*Schmitt et al.*, 2016), which constitutes the topic and the main tool used for this thesis.

The CASCADE modelling framework allows to simulate transport of sediment mixtures originating from multiple sources combining concepts of graph-theory and sediment transfers. It aims to analyse sediment connectivity at the network scale and so include the evaluation of sediment transport processes in IWRM (Integrated Water Resources Management, *Soncini-Sessa et al.* (2007)), particularly in dam siting problems (*Jager et al.*, 2015). The reduction of sediment fluxes downstream of dams may indeed have impacts both on the downstream reaches, subject to major erosion, and also on the overall connectivity at the network scale (*Schmitt*, 2016).

1.1 Literature review

Sediment connectivity involves multiple spatio-temporal scales: solid transport models have been widely developed at the single reach scale, but studying sediment connectivity still represents a challenge. Different approaches to model sediment connectivity have been experimented.

Common hydrologic models (e.g. SWAT) can be used to model transport of suspended sediment loads (as described by *Betrie et al.* (2011) and *Ranzi et al.* (2012)), but computational time rises at larger scales. On the other hand hydraulic models at the network scale (e.g. Mike 11, HEC-Ras) require too detailed wide-spread input data to characterise the river morphology. This, together with high computational costs, prevents their use on large basins (*Merrit et al.*, 2003).

Prediction of channel tendency towards aggradation or incision have been proposed based on stream power assessments by *Bizzi and Lerner* (2015) and *Parker et al.* (2015). Spatio-temporal flux simulations deriving from sediment mass balances along a sediment cascade have been analysed by *Benda and Dunne* (1997) as a result of stochastic activation of sediment sources. A similar approach was used also to predict reaches subject to sediment deposition within a river network (*Wilkinson et al.*, 2006).

Czuba and Foufoula-Georgiou (2014) were the first to adopt a graph-theoretic approach implementing individual sediment transport processes, which allowed to simulate trajectories of single sediment loads (*Czuba and Foufoula-Georgiou*, 2015). Still sediment mass balances are not calculated for each reach, which prevents from deriving actual transport rates or information on where sediment from a certain source deposited (*Schmitt*, 2016).

All these studies miss to quantify disaggregated information about provenance and destination of single sediment loads, which is the main innovative aspect of CASCADE model (*Schmitt et al.*, 2016). This is allowed by the simulation of individuals transport processes of single specific grain size sediment loads, resulting in global fluxes composed of various grain sizes throughout the river network. Sediment transport phenomenon can be thus analysed from both a source and a sink perspective, tracing and quantifying all trajectories of fluxes starting from a source reach or incoming to a reach from different sources respectively.

1.2 Objectives of the thesis

CASCADE model is thought to be implemented using easily accessible information on the basin topography, such as a digital elevation model (DEM), and hydrological data available through local network of monitoring gauging stations. For this reason, the model is suitable to simulate major basin with scarce data, as in the case of previous implementations of CASCADE model (*Schmitt et al.* (2015), *Schmitt et al.* (2015a), *Bizzi et al.* (2016) and *Schmitt et al.* (2016a)), yet a proper validation based on a detailed dataset is missing. New applications should be then developed using accurate information in order to more thoroughly test CASCADE performances and verify its actual accuracy and potentiality. For this sake, the Piedmont case study offers the possibility to use information generated from a previous work focused on river hydromorphological characterisation using Remote Sensing data (*Demarchi et al.* (2016) and *Demarchi et al.* (accepted)), which provides a dataset on channel characteristics densely available for the main rivers of Piedmont. In addition to hydromorphological data, also assessments of bed load sediment transport and superficial surveys of grain sizes are available on various locations from previous studies, allowing a validation of the CASCADE performances more exhaustive compared to the previous model applications. Moreover most of these applications focused on sandy rivers, so the Upper Po river

network, largely dominated by gravel, provides an opportunity to test the model also in different grain size conditions.

Besides presenting the study site application, this work represents also a first attempt to formalise the MATLAB framework which underpins CASCADE, in order to introduce key aspects about the conceptualisation of processes and MATLAB components necessary to carry out the simulation and for the elaboration of final outputs. Particular attention is paid to the MATLAB implementation of the several modelling components, for an overall knowledge of the basic functioning and characteristic variables is essential to extract information of interest from the outputs of the simulation. Moreover, an additional component for extracting and characterising the river network object of the simulation was specifically elaborated and added to the modelling framework.

Main objectives of this thesis are therefore two:

1. implementing CASCADE for the main river network of the Upper Po River in the Piedmont Region, where accurate data are available for both the calibration and the validation of the model;

2. providing a conceptualisation and formalisation of the Matlab framework underpinning CASCADE.

1.3 Outline of the thesis

In chapter 2 CASCADE model is presented both on a conceptual and a practical level, describing the basic functioning and its implementation in MATLAB environment. Chapter 3 is dedicated to the implementation of the Upper Po basin case study, describing in detail the preprocessing of input data and the new MATLAB tools used to obtain the river network necessary for the CASCADE simulation. Results of the simulation are presented in chapter 4 and compared to available validation data. Finally, after conclusions and future development discussed in chapter 5, in the appendix a list of used symbols and tables for cited MATLAB functions and scripts are provided.

CHAPTER 2

CASCADE model

CASCADE (**CA**tchment **S**ediment **C**onnectivity**A**nd **DE**livery) modelling framework is a newly developed modelling approach for the sediment connectivity analysis at the river network scale. It has been designed by Rafael J. P. Schmitt during his PhD and it is currently a research topic of the group on natural resource management at the Dipartimento di Elettronica, Informazione e Bioingegneria (DEIB) of Politecnico di Milano.

In this chapter, CASCADE model is presented both on a conceptual and a practical level, describing the basic functioning and its implementation in MATLAB environment. As for theoretical aspects, reference is made to *Schmitt et al.* (2016) using the same notation (presented in section 2.1.2 of this chapter and in section .1 of the appendix), whereas MATLAB scripts and functions presented and applied in this work are listed in tables 1 and 2 of the appendix.

2.1 Introduction to CASCADE modelling framework

2.1.1 CASCADE basic functioning and key concepts

CASCADE modelling framework aims to simulate sediment fluxes throughout a river network by implementing multiple *cascades*. A cascade is defined as an individual transport process of a single specific grain size sediment load originated from a precise source in the river network. Figure 2.1 illustrates the basic concepts of the modelling approach.

The physical river network has to be represented by a direct acyclic graph composed by nodes and edges, as shown in figures 2.1(a) and 2.1(b). Nodes are roughly located at a standard distance from each other and at river confluences. Every edge represents a river stretch, herein called *reach*, in each of which multiple cascades can both originate by sediment detachment or travel along, potentially losing a portion of the original sediment load by deposition.

Sediment detachment phenomenon occurring in every reach is represented by one or more sediment sources, each giving rise to a cascade. Cascade sources, identified in the figure by roman numbers, are characterised by a certain supply and by a specific grain size (the latter highlighted through the dot size in figure 2.1(c)) according to the material present in the bed river and banks of the reach in which the source is located.

Cascade sources illustrated in figure 2.1(c) give rise to cascades in figure 2.1(d), which deliver downstream their own specific grain sizes. Figure 2.1(d) shows also how multiple cascades can be active along a reach, delivering in parallel multiple sediment loads of different grain size. Sediment loads carried by different cascades remain conceptually separated and distinguishable even if transported simultaneously through the same reach.

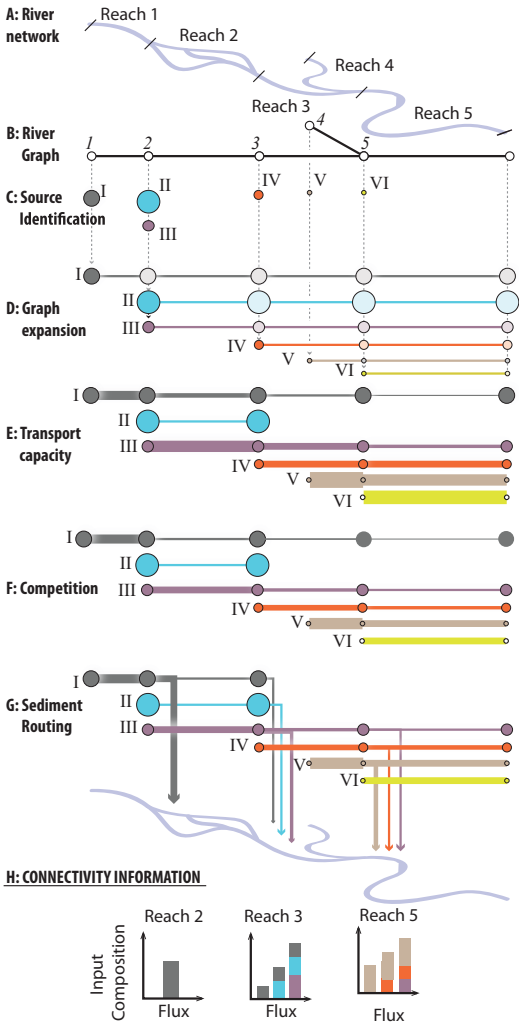

Figure 2.1: *Key concepts and steps behind the CASCADE modelling framework. A and B: original river network and graph representation. C: identifying source locations and grain sizes. D: graph expansion. E: transport capacity scaling, line width indicates transport capacity. F: competition reduces the original transport capacity (compare line width in E and F). G: cascade specific, edge-to-edge sediment routing discriminates cascade sediment fluxes. H: edges receive fluxes from multiple cascades, defining sediment flux, provenance, and sorting; and thereby connectivity of an edge. (Figure edited from Schmitt et al. (2016))*

Every cascade is uniquely identified by its source, where it receives the one and only sediment contribution. This is necessary to have only unique source-sink relationships, from which connectivity information can be derived both from a sink and a source point of view. After the initial supply, the sediment load transported by a cascade will not receive additional contributions then, so it can only decrease due to deposition. Not the whole sediment load is entrained downstream of each reach indeed, because the flow energy may be locally insufficient and the amount that cannot be transported is deposited. To quantify these fractions of sediment load being deposited or entrained downstream, also the available flow energy need to be quantified then. Each cascade is assigned in every reach a certain amount of energy available for sediment entrainment, called *transport capacity*, visualised by the line width in figure 2.1(e). Transport capacity is calculated by applying empirical sediment transport formulas based on the transported grain size, local morphology and local hydraulic forcing. These local variables determine for the same cascade different values of transport capacity in every reach along its pathway, hence the varying line width within a cascade displayed in figure 2.1(e). Moreover transport capacities of a cascade depend on its specific grain size, as just mentioned. Under the same local conditions, cascades carrying finer grain sizes are assigned higher transport capacities, as visible for instance in figure 2.1(e) from the comparison of cascades I and III: the line width of cascade III is always larger than cascade I for the same reach, since the grain size delivered by III is finer.

Such transport capacities however represent the hypothetical energy available for a cascade crossing a reach if no other cascades were also present. The presence of multiple cascades crossing the same reach implies a certain allocation of the flow energy between cascades. This is represented in CASCADE modelling framework through the concept of competition, which causes a reduction of the available energy for all the cascades, which is evident by the comparison of figures 2.1(e) and 2.1(f).

Finally, each cascade is simulated quantifying sediment fluxes crossing every reach. Competition corrected transport capacities are used to define how much of the incoming sediment flux can be entrained downstream reach per reach. If the local transport capacity is insufficient to transport downstream the whole sediment flux incoming from upstream, then a certain part is deposited, as illustrated by downwards arrows in figure 2.1(g). If the transport capacity is insufficient to entrain at all the cascade specific grain size through a reach, then the cascade is definitively interrupted (as for cascade II displayed in figure 2.1(e), for instance). An interruption of the delivery process may occur also if the cascade has exhausted its initial load due to deposition along its pathway (e.g. cascade I in figure 2.1(g)), or in case a reservoir is present. If not interrupted before, cascades will deliver a certain amount of sediment, generally less than or at most equal to the initial supply, up to the basin outlet.

2.1.2 Conventions and symbols

All nodes are identified by a unique identification code and reaches are named after their upstream nodes.[1] In the version of the model presented in this work one and only one cascade source per reach is defined, so identifiers of sources coincide with identifiers of reaches (under this hypothesis, in figures 2.1(b) and 2.1(c) there would be perfect correspondence between Roman numerals identifying sources and Arabic

[1] The only exception is at the outlet, referred to as Ω, where the edge and the two endpoint nodes have the same identifier.

numerals identifying reaches). Therefore in the following only reach identifiers will be used and so each source, and hence each cascade too, will be identified by the reach in which the source is located.

Every reach is at once a source for one cascade and a part of the pathway for multiple cascades. The symbol ς is here used to refer to a generic reach when seen as a source for a cascade, which will be named γ_ς after it. On the other hand the symbol e (standing for "edge") is used when referring to a generic reach in the function of sink, which is not to be intended as the end of the cascade, but in more general terms as a reach crossed by a cascade along its pathway (the latter referred to as κ_ς in turn). Each cascade transports a specific grain size d_ς, depending on the available material at the source reach ς.

Key quantities such as transport capacity (denoted with Q_S), or sediment fluxes Θ, shall be referred to a specific cascade γ_ς in a specific reach e, so for instance $Q_{S_e^\varsigma}$ is the transport capacity of cascade γ_ς in reach e. The MATLAB implementation of such variables will be discussed in section 2.2.2. Some others quantities may also be referred just to a single reach, so for instance the flux Θ_e is the total sediment flux crossing reach e, resulting from the summation of fluxes Θ_e^ς of all cascades such that $\gamma_\varsigma \in \Gamma_e$ (i.e. the set of all cascades crossing reach e).

2.1.3 Flow chart

In figure 2.2 a flow chart is provided to illustrate the several modelling components included in CASCADE modelling framework and the main variables relating them. Symbols used for the latter are clarified in table 2.1.

CASCADE model requires input information about river network (derived from a digital elevation model), channel widths and hydrology. More in detail, hydrological information consist in a set of observed hydrographs $\boldsymbol{Q_{SB}}$, which need to be downscaled to derive estimated local hydrographs $\boldsymbol{Q_e}$.

Local hydrological information is used on the one hand to simulate bankfull hydraulics, in which the *grain size solver* estimates cascades' grain sizes d_ς, and on the other hand it is needed to calculate transport capacities $Q_{S_e^\varsigma}$. $Q_{1.5_e}$ is the 1.5 year discharge, providing an estimate of the bankfull discharge, whereas for transport capacity calculations single discharges $Q_e(p)$ are used, synthetically representing the total hydrograph $\boldsymbol{Q_e}$. [2] In both cases discharge values are turned into water levels h and flow velocities v by the *hydrodynamic solver* based on local morphological features (i.e. slope I_e and width W_{ACe}).

Grain sizes d_ς in source reaches $e = \varsigma$ supplying cascades γ_ς are calculated from bankfull hydraulics $h_{1.5,e}$ and $v_{1.5,e}$ and source reaches' morphology.

Transport capacities $Q_{S_e^\varsigma}$ are calculated for each cascade γ_ς through empirical formulations based on grain size d_ς, morphological features in each reach e and local hydraulics $h_e(p)$ and $v_e(p)$ corresponding to percentile-defined classes p.

To take into account competition between cascades crossing at once the same reach, corrected transport capacities $Q_{S_e^{\varsigma\prime}}$ can be calculated according to 4 different alternative competition scenarios. A reference transport capacity $Q_{S_e}(d_{50e})$ (based on the median grain size d_{50e} expected in each reach e) is involved in scenarios 1 and 2, whereas

[2] To compress hydrological information, each hydrograph $\boldsymbol{Q_e}$ is dissected by $p+1$ percentiles into p discharge classes, whose central values are discharges $Q_e(p)$, as will be discussed in section 2.6.

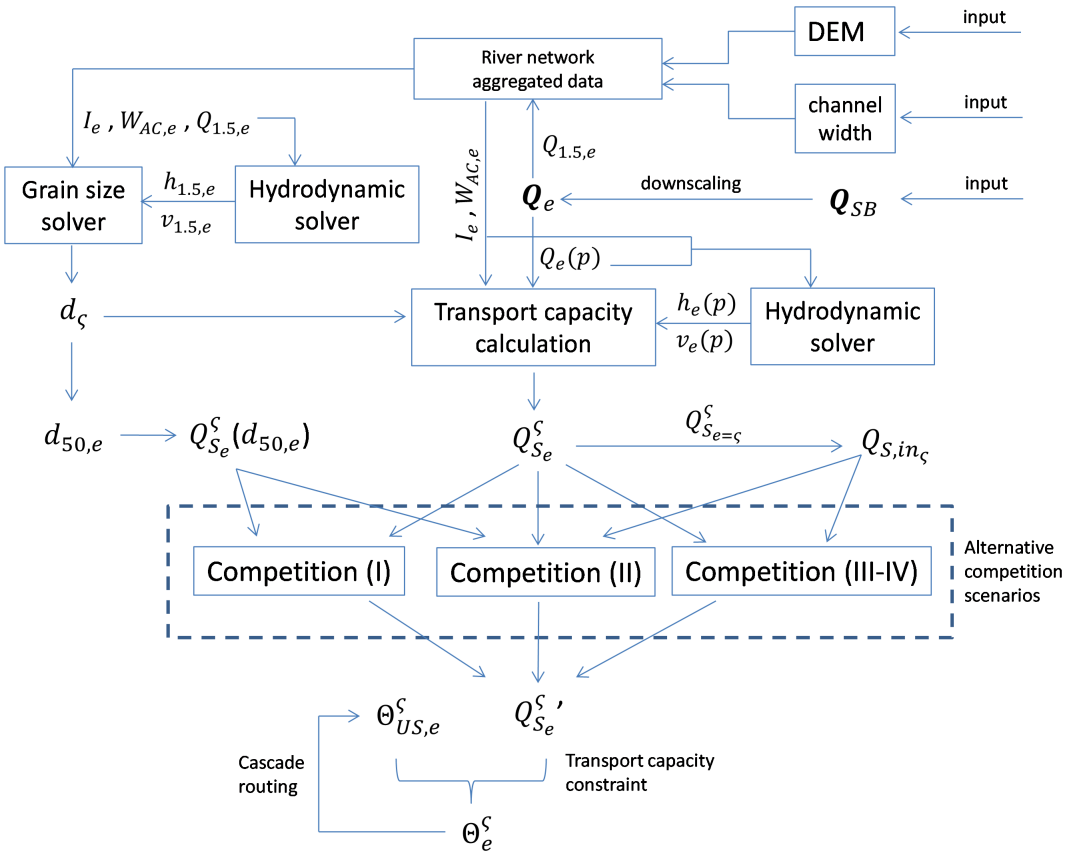

Figure 2.2: *Flow chart of CASCADE modelling framework*

Symbol	CASCADE variable
d_ς	grain size assigned to source ς, transported by cascade γ_ς
d_{50e}	median grain size expected in reach e
$h_{1.5,e}$	bankfull water level in reach e
$h_e(p)$	water level in reach e related to percentile-defined class p
I_e	mean slope of reach e
p	discharge percentile-defined class
$\boldsymbol{Q_e}$	estimated hydrograph for reach e
$\boldsymbol{Q_{SB}}$	observed hydrograph related to sub-basin SB
$Q_{1.5_e}$	1.5 year discharge estimated for reach e, approximating bankfull discharge
$Q_e(p)$	central value within percentile-defined discharge class p related to reach e
$Q^\varsigma_{S_e}$	transport capacity related to cascade γ_ς in reach e
$Q^{\varsigma\prime}_{S_e}$	corrected transport capacity related to cascade γ_ς in reach e
$Q_{S_e}(d_{50e})$	reference transport capacity for reach e based on the expected median grain size d_{50e}
Q_{S,in_ς}	initial supply of cascade γ_ς
$v_{1.5,e}$	bankfull flow velocity in reach e
$v_e(p)$	flow velocity in reach e related to percentile-defined class p percentile-defined class
W_{ACe}	active channel width of reach e
Θ^ς_e	sediment flux of cascade γ_ς entrained through reach e
$\Theta^\varsigma_{US,e}$	sediment flux of cascade γ_ς incoming from upstream into reach e

Table 2.1: *Flowchart variables*

the initial supply Q_{S,in_ς} (set equal to the transport capacity value in the source reach $Q_{S_{e=\varsigma}{}^\varsigma}$) is used in scenarios 2,3 and 4.

Finally, each cascade γ_ς is routed from the source ς to downstream through implementing reach-to-reach mass balances, where the sediment flux Θ_e^ς entrained through a reach e depends on the upstream incoming flux $\Theta_{US,e}^\varsigma$ and the local corrected transport capacity $Q_{S_e^\varsigma}{}'$.

2.2 Introduction to MATLAB implementation

2.2.1 Coding

Modelling components described through the flowchart presented in the previous section are implemented through specific MATLAB scripts and function, which will be presented along this chapter by referring to a particular version of CASCADE coding, suitable to simulate sediment fluxes in an undisturbed state (i.e. without considering the effects of reservoirs, although generally relevant), with no supply limitation for cascade sources, and with one and only one cascade source per reach. Nevertheless, CASCADE model is meant to be developed into newer versions allowing also to consider the presence of reservoirs, impose a sediment supply limit and initialise multiple cascade per reach, as will be discussed in general terms throughout the present chapter.

The version of CASCADE's code described in detail in this chapter was applied to the case study described in chapter 3 for the simulation of sediment fluxes over the Piedmont river network under the assumptions cited above.

The MATLAB functions and scripts cited in this thesis and applied to the case study are listed in table 1, grouping the coding within CASCADE modelling framework (*Schmitt et al.*, 2016), and 2, grouping all functions and scripts specifically developed for the case study simulation implemented in this work. Both the tables can be found in section .2 of the appendix.

2.2.2 Variables implementation

As already mentioned in section 2.1.2, some quantities related to cascades also depend on local conditions, so they need to be referred at once to a specific cascade γ_ς and a specific reach e. According to the notation introduced, the symbol α_e^ς is used to identify a generic feature α related to the cascade γ_ς while crossing reach e.

Variables representing such cascades' quantities varying over reaches are implemented in the form of origin-destination matrices, where rows are referred to cascades sources (origins) and columns to reaches crossed by cascades (destinations). Let's now assume that the hypothetical feature α is represented through a matrix A: a generic element $a_{i,j}$ located in the i^{th} row and j^{th} column of matrix A contains a value referred to a cascade originating in the reach corresponding to the i^{th} row of the matrix when crossing the reach corresponding to the j^{th} column of the matrix.

According to their definition, the number of columns of these origin-destination matrices will always be equal to the total number of reaches in the river network, representing all possible reaches along a cascade pathway where sediment loads can either pass through or deposit. Rows of matrices are instead referred to cascade sources, and so to cascades. If multiples sources are defined per each reach, the number of rows

may be greater than the total number of reaches: being the latter equal to number of columns, in this case matrices are generally rectangular.

In case of one and only one cascade source per reach (as for the code version presented here and applied for the case study described in chapter 3) matrices are square of size equal to the total number of reaches in the river network, being every reach a source for only one cascade and potentially a destination or a part of the pathway for all other cascades. In this version of CASCADE code the identification number of a reach matches its ordinal number in a vector or a matrix[3] so, according to the previous example, the variable α_e^{ς} referred to cascade γ_{ς} crossing reach e is represented by the element $a_{i=\varsigma,j=e}$ located in the ς^{th} row and e^{th} column of matrix A.

If a reach e of the graph is not topologically connected to a certain source ς, then element $a_{\varsigma,e}$ will be void. All elements in the ς^{th} row refer to a cascade γ_{ς} originating in reach ς (potentially crossing several reaches, i.e. all non-void elements of that row). In the same way, all elements in the e^{th} column refer to a single reach e (potentially crossed by several cascades, i.e. all non-void elements of that column).

2.3 Input data

Main inputs required by CASCADE model consist in a graph representation of the river network and the characterisation of related reaches in terms of morphological properties and hydrological observations over a certain time horizon.

2.3.1 River network

CASCADES models fluxes of sediments within a river network, which has to be represented by a graph of nodes and edges, representing river reaches. The graph information is to be provided through a matrix, called `AggData` in the MATLAB code, in which every row refers to a reach in the graph. The matrix has to be composed by the following columns:

1. Reach identification code;
2. Upstream node (called also "From Node") identification code, equal to reach identification number;
3. Downstream node (called also "To Node") identification code;
4. Upstream node elevation $[m]$;
5. Downstream node elevation $[m]$;
6. Reach mean slope $[-]$;
7. Reach length $[m]$;
8. Reach Strahler order;
9. Drainage area of the reach (conventionally set equal to the drainage area of the upstream node) $[km^2]$;
10. East coordinate of upstream node $[m]$;
11. North coordinate of upstream node $[m]$;

[3]This is possible because there is one and only one cascade source per reach, so the total number of source reaches (rows in matrices) and reaches as part of pathways (columns in matrices) is the same. This allows to sort the list of total reaches by their identification numbers, in order to make them match their ordinal number in the list. This list can be seen as the vector of indices of both rows and columns in origin-destination matrices. Therefore here and in the following no difference will be made between identification code of a reach and its ordinal number in a vector or a matrix.

12. East coordinate of downstream node $[m]$;
13. North coordinate of downstream node $[m]$;
14. Active channel width of the reach $[m]$.

As already mentioned in the previous section, identifiers of reaches match their position in the matrix, so for instance the e^{th} row of matrix `AggData` is referred to reach e.

Section 3.2.1 will be dedicated to describe how such a matrix has been calculated for the Piedmont case study on the basis of terrain elevation and channel width data.

2.3.2 Hydrologic data

Raw hydrological information required in input by CASCADE is provided through a set of observed hydrographs, denoted by the symbol $\boldsymbol{Q_{SB}}$. Observed hydrographs consist in daily discharge time series registered in gauging stations spread over the river network over the same time horizon and have to be stored in the MATLAB table `hydrologicData`, where:
- the first column contains the progressive numeration of days in the time horizon;
- the second columns contains related dates;
- the third column contains daily discharges for the concerned gauging station.

For each gauging station, identified by a name and a code, also drainage areas and local coordinates are to be provided, which are needed for the assignment to river network reaches that will be described in section 3.3.1 for the Piedmont case study.

2.4 Preprocessing

In this section the preprocessing of previously described inputs is discussed. Main modelling components and variables involved are highlighted in the flow chart of figure 2.3.

Graph preprocessing

In the section `graph preprocessing` of the main script raw network data contained in matrix `AggData` are preprocessed in order to derive topological information, such as lists of reaches upstream or downstream of each reach. This kind of information is then stored into structure `Network`. Based on this structure, other important variables concerning network topology are derived:
- matrix `II`, in which the (i, j) element represents the topological distance from reach i to reach j;
- scalar `outlet_node`, i.e. the identification code of the river network outlet;
- vector `US_hierarchy`, whose elements contain the number of downstream reaches up to the outlet for every reach.

Slope correction

Slopes contained in `Network` may need to be preprocessed in order to correct non-valid slopes (i.e. with non-negative gradient towards flow direction) due to any inaccuracies in raw elevation data. In the section `Correct slopes` of the main script the function `slope_correction` is used to fix such problems.

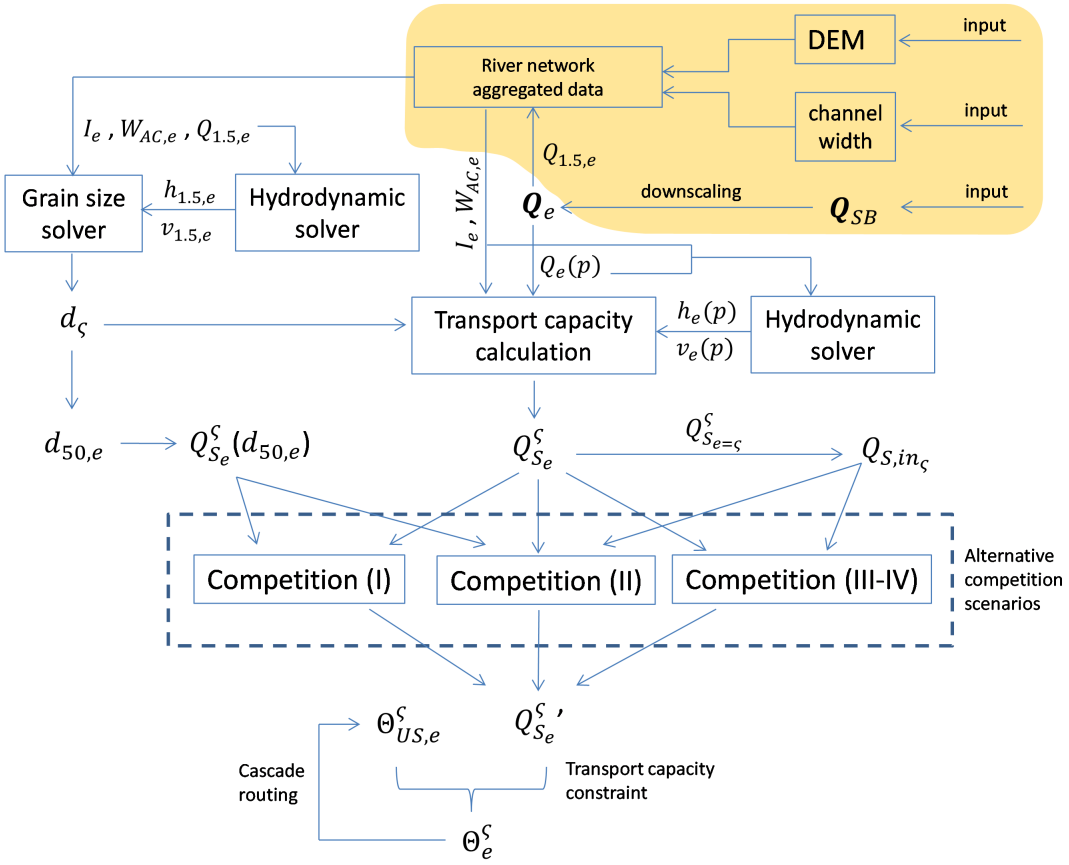

Figure 2.3: *Components and variables involved in the preprocessing phase described in section 2.4. CASCADE model requires input information about river network (derived from a DEM), channel widths W_{AC} and hydrology. Hydrological information consists of a set of observed hydrographs $\boldsymbol{Q_{SB}}$, from which 1.5 year discharges are derived and used to calibrate a regression on drainage areas. The regression is then applied to estimate in every reach e the 1.5 year discharge $Q_{1.5_e}$, to be aggregated to river network data.*

Hydrologic data

In the section `Process hydrologic data` of the main script raw input hydrographs (stored in the MATLAB table `hydrologicData` as described in section 2.3.2) are preprocessed to get all information required for following hydraulic calculations, to be stored in the cell array `Q_data`. In particular, the gauging stations in which observed hydrograph were measured need to be associated to reaches of the river network graph.[4] From every observed hydrograph $\boldsymbol{Q_{SB}}$ (where SB stands for the sub-basin closed at the gauging station) is then extracted the percentile $Q_{1.5SBe}$ corresponding to the return period of 1.5 year. The 1.5 year discharge provides a good approximation of the bankfull discharge (*Knighton*, 1984) , which will be used in section 2.5 for the grain size initialisation and in section 2.6 to extend local hydrological information measured at gauging stations to the whole river network. At this stage $Q_{1.5SBe}$ is used to calibrate a power law regression on the gauging station drainage area $A_{D_{SB}}$

$$Q_{1.5SB} = a * {A_{D_{SB}}}^b \tag{2.1}$$

[4]This operation is described in detail for the Piedmont case study in section 3.3.1

which is needed to derive an estimate of $Q_{1.5e}$ in every reach e by applying the regression on drainage area A_{De}

$$Q_{1.5e} = a * {A_{De}}^{b} \tag{2.2}$$

using the same parameters a and b just calibrated using gauging stations data. $Q_{1.5e}$ is then stored in matrix `AggData` in an additional column identified by `ID_Q15`.

At the end of this phase results are stored in cell array `Q_data`, whose columns refer to gauging stations and rows contain:

1. name of the gauging station;
2. identification code of the closest reach e_{SB} in the river network;
3. observed hydrographs $\boldsymbol{Q_{SB}}$ (time series discharge in $m^3\ s^{-1}$);
4. 1.5 year discharge $Q_{1.5SB}$ $(m^3\ s^{-1})$;
5. area of the sub-basin SB closed at the gauging station $A_{D_{SB}}$ (km^2).

Once each gauging station's sub-basin SB has been associated to a reach e_{SB} in the graph, then it is possible to assign to every reach e of the river network the gauging station's sub-basin SB_e within which e is located. This basically consists in choosing the next gauging station downstream of that reach by exploiting topological information contained in structure `Network`. So every reach e is assigned a reference gauging station within the same sub-basin SB_e and a reference hydrograph $\boldsymbol{Q_{SBe}}$, which will be used in section 2.6 to derive hydrological information in every reach. Belonging to the same sub-basin, discharge frequency and magnitude information provided by the observed reference hydrograph will be similar to those of the local hydrograph to be estimated. The identifier of the reach representing the location of the reference gauging station SB_e for every reach e is then stored in matrix `AggData` in a new column identified by `ID_WSID`.

2.5 Grain size solver

In this section the initialisation of cascades' grain sizes, performed by the *grain size solver*, is described. Main modelling components and variables involved are highlighted in the flow chart of figure 2.4.

Sediment loads carried by each cascade derive from sediment detachment locally occurring in the source reach ς, so the grain size d_ς transported by cascade γ_ς depends on the kind of the material locally present in the bed river and banks. Ideally d_ς should be set based on local measurements in every reach, which generally are not available though. For this reason CASCADE model provides a grain size solver to obtain an approximate estimate of a single grain size per source reach based on local hydrological conditions.[5] In detail, characteristic grain size d_ς is calculated as the equilibrium grain size established under bankfull hydraulic conditions. This method is based on the hypothesis that only the largest fractions of the grain size mixture in a source reach ς

[5] As already mentioned, in the version of CASCADE code herein presented only one cascade per reach is routed, so every reach of the graph is the source ς of a single cascade γ_ς, carrying a load of sediment of a single grain size d_ς which can be then estimated by the grain size solver.

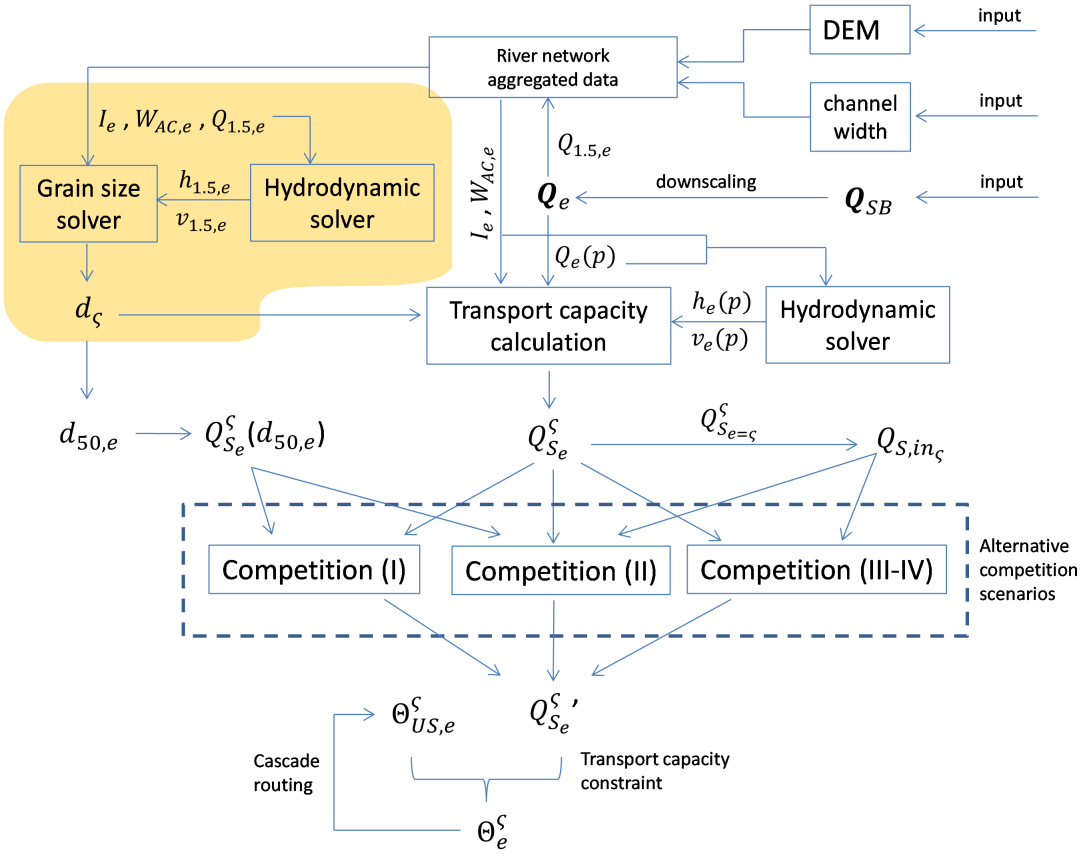

Figure 2.4: *Components and variables involved in calculations performed by the grain size solver described in section 2.5: Grain sizes d_ς in source reaches $e = \varsigma$ supplying cascades γ_ς are calculated from local morphology (i.e. slope I_e and width W_{ACe}) and bankfull hydraulics $h_{1.5,e}$ and $v_{1.5,e}$ (derived from $Q_{1.5_e}$ by the hydrodynamic solver).*

are not mobilised under bankfull flow conditions, while finer sediments are entrained downstream by the flow (*Andrews*, 1983).

Bankfull hydraulic conditions in every source reach ς are simulated by the grain size solver based on $Q_{1.5_e}$, that is the local 1.5 year discharge approximating bankfull discharge, previously derived through the power law regression described by equation (2.2) in section 2.4.

The grain size solver is implemented through function `hydraulicCalc`, which receives as input matrix `AggData`, containing reach properties, and returns the output matrix `hydraulicData` containing bankfull hydraulics and equilibrium grain sizes for every reach.

The equilibrium grain size is derived by the grain size solver as a function of local slope I_e and from the hydraulics $v_e(Q_{1.5})$ and $h_e(Q_{1.5})$, i.e. local water level and flow velocity under bankfull conditions. Bankfull hydraulics $v_e(Q_{1.5})$ and $h_e(Q_{1.5})$ are derived from the $Q_{1.5_e}$ (stored in column `ID_Q15` of matrix `AggData`) through the *hydrodynamic solver* based on local slope I_e and active channel width W_{ACe}, assuming for the section a rectangular shape. The hydrodynamic solver, displayed in the

flowchart in figure 2.4, is an iterating procedure solving for the water level h_e. Iterations are based on the minimisation of an objective function, defined through function `hydraulicSolver` as the absolute difference between $Q_{1.5_e}$ and the discharge calculated as function of water level h_e.

Resulting hydraulics give rise to the critical shear stress defining the equilibrium grain size established under bankfull conditions. The calculated shear stress however is referred to the bed of the river, assuming thus that sediment detachment occurs only from bed-river and not from banks.

In the end function `parameterToMatrix` is used to derive matrix `Dmat` based on the vector of calculated diameters d_ς and topological information contained in matrix `II` (see 2.4). This operation results in assigning to every element of matrix `Dmat` the grain size d_e^ς (ς^{th} row, e^{th} column) transported by cascade γ_ς in reach e: for every cascade γ_ς (and so every row of the matrix) the transported grain size d_ς is assigned for all reaches belonging to the cascade pathway κ_ς^Ω (corresponding to a certain set of columns in the selected row). The vector of grain size sources initialisation constitutes the main diagonal of matrix `Dmat`, for which $e = \varsigma$.

2.6 Hydraulic calculations and derivation of transport capacities

This section is dedicated to the derivation of transport capacities and to the preparatory hydrological and hydraulic calculations, synthetically illustrated by figure 2.5 and encoded by MATLAB script `HydraulicCalcs`.

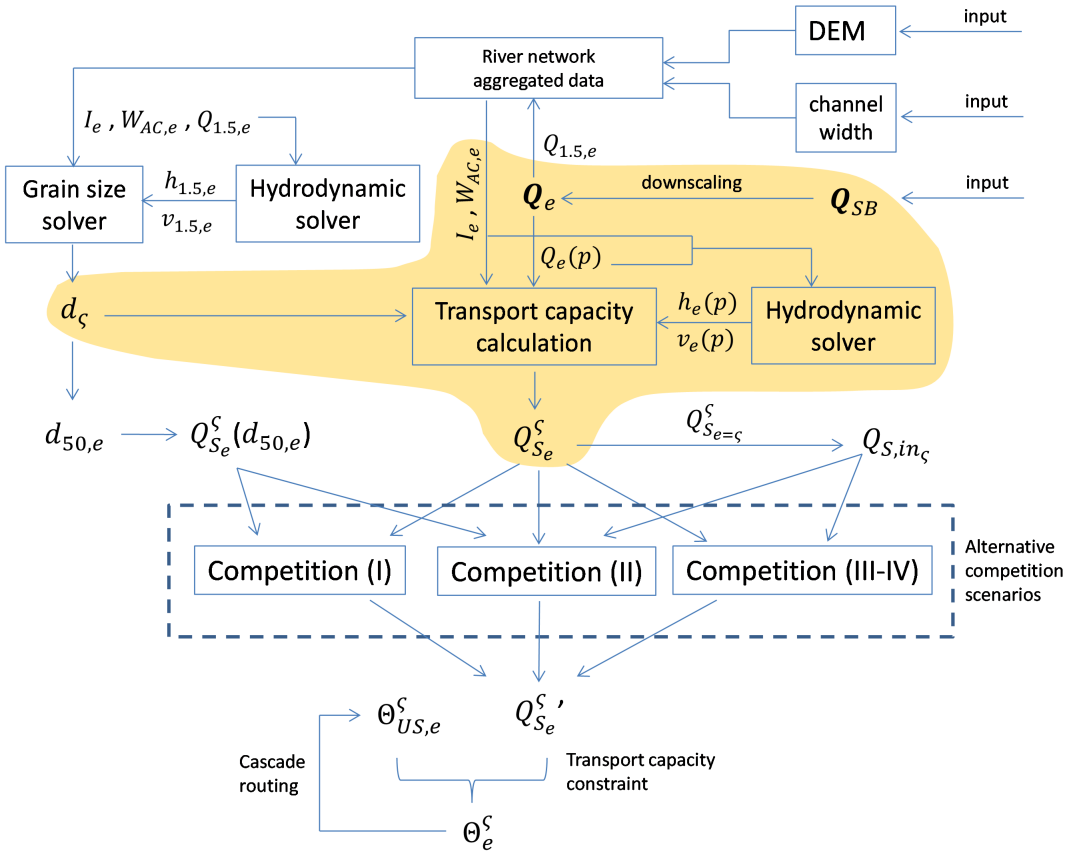

Figure 2.5: *Components and variables involved in hydraulic calculations and derivation of transport capacities described in section 2.6. Observed hydrographs $\boldsymbol{Q_{SB}}$ in input need to be downscaled to derive estimated local hydrographs $\boldsymbol{Q_e}$. Each local hydrograph $\boldsymbol{Q_e}$ is then dissected into percentile-defined classes p, in which discharges $Q_e(p)$ are the mean values for which transport capacity calculations are performed for each reach e. Transport capacities $Q_{S_e^\varsigma}$ are then calculated for each cascade γ_ς through empirical formulations based on grain size d_ς, morphological features (I_e and $W_{AC\,e}$) and local hydraulics $h_e(p)$ and $v_e(p)$, derived by the hydrodynamic solver and corresponding to the percentile-defined classes p.*

To calculate transport capacities $Q_{S_e^\varsigma}$ CASCADE needs hydrological information in every reach based on locally observed hydrographs, which are available only in a limited number of gauging stations. Therefore observed hydrographs need to be scaled to obtain a local hydrograph for each reach. This process is implemented in the first part of script `HydraulicCalcs`.

Observed hydrographs $\boldsymbol{Q_{SB}}$ and 1.5 year discharges $Q_{1.5SBe}$ are stored in cell array `Q_data`, obtained in the preprocessing described in section 2.4.

To implement the downscaling from observed hydrographs to local hydrographs, a multiplicative scaling factor J_e is calculated for each reach as ratio of the 1.5 year

discharge of the local reach $Q_{1.5e}$ to the 1.5 year discharge observed at the next downstream gauging station $Q_{1.5SBe}$:

$$J_e = \frac{Q_{1.5e}}{Q_{1.5SBe}} \tag{2.3}$$

where $Q_{1.5e}$ is the local 1.5 year discharge derived through the power law regression described by equation (2.2) in section 2.4, stored in column `ID_Q15` of matrix `AggData`.

Equation (2.3) for the the scaling factor J_e can be therefore rewritten as

$$J_e = \frac{a * {A_{De}}^b}{Q_{1.5SBe}}. \tag{2.4}$$

Once the scaling factor is calculated, the whole local hydrograph $\boldsymbol{Q_e}$ can be derived by multiplying the scaling factor by the reference observed hydrograph $\boldsymbol{Q_{SBe}}$:

$$\boldsymbol{Q_e} = J_e \cdot \boldsymbol{Q_{SBe}}. \tag{2.5}$$

The reference observed hydrograph $\boldsymbol{Q_{SBe}}$ to be downscaled for each reach e is specified in column `ID_WSID` of matrix `AggData`, containing for every reach e the identifier of the reach in which the reference gauging station SB_e is located.

To compress hydrological information, each hydrograph $\boldsymbol{Q_e}$ is dissected into p discharge classes by $p + 1$ percentiles, so that central values of classes $Q_e(p)$, together with their frequencies $n_e(p)$, represent the whole hydrograph. This allows to execute following calculation only for a small number of discharge values saving computational time. Herein each hydrograph has been dissected into 8 discharge classes by 9 percentiles, defined in order to be spaced of one standard deviation paces from -4σ to $+4\sigma$ in a normal standard distribution (so corresponding probability values are 0.1%, 2.3%, 15.9%, 50%, 84.1%, 97.7%, 99.9%). Such σ-intervals allow to consider the potential effect on sediment transport of rare, but high magnitude flow events (e.g., *Wolman and Miller* (1960)).

Assuming uniform distribution of observations within every discharge class, central values $Q_e(p)$ can be considered the mean discharge values of each class.

Local hydraulics $h_e(p)$ and $v_e(p)$ corresponding to all mean discharges $Q_e(p)$ in percentile-defined classes p are derived by the hydrodynamic solver, already described in section 2.5 dedicated to the grain size solver, when it was used to derive bankfull hydraulics from 1.5 year discharges.

Output variables of this phase are stored in cell array `stats`, where columns refer to reaches and columns contain:

1. Hydrograph scaling factor J_e;
2. Percentile values according to a normal distribution;
3. Vector containing mean discharges $Q_e(p)$ within each discharge class p;
4. Vector containing numbers of observations $n_e(p)$ for each discharge class p;
5. Vector containing mean waters levels $h_e(p)$ for each discharge class p;

6. Vector containing mean flow velocities $v_e(p)$ for each discharge class p;
7. Total number of days on record n_{tote}.

Transport capacity calculation

Transport capacity, denoted by the symbol Q_S, is a metric used to define the maximum sediment flux in terms of $kg\ yr^{-1}$. Transport capacities are always referred to a specific cascade γ_ς and to a specific reach e, so a generic $Q_{S_e}^{\varsigma}$ defines the highest possible annual transport rate of sediments through e for γ_ς.

Transport capacity basically depends on the carried grain size and on hydro-morphological local conditions, under which it quantifies how much sediment of that size can be entrained per year by the river flow energy.

The sediment transport process is different for the various grain size classes: clay and fine silt are transported as suspended load, gravel and cobble as bed-load, whereas sand is transported either in suspension or on the river bed based on local hydraulics. This results in different formulations involved in the calculation of transport capacity:

- Engelund and Hansen formulation, for grain size finer than 2 mm (mainly sand) (*Engelund and Hansen*, 1967);
- Wong and Parker formulation, for grain size coarser than 2 mm (mainly gravel) (*Wong and Parker*, 2006).

At first calculations are presented describing how to derive the local transport capacity of a single cascade γ_ς in a reach e and after that the discussion will address the MATLAB function implementing the calculation for every cascade in every reach.

As stated above, $Q_{S_e}^{\varsigma}$ depends on the grain size d_ς and on local hydrology and morphology. In particular the local hydrograph $\boldsymbol{Q_e}$ provide information about magnitude and frequency of discharges estimated in reach e over the time horizon in which data are collected. Based on discharges, water levels h_e and flow velocities v_e can be derived. As regards local morphology, the metrics of interest are the slope I_e and active channel width W_{ACe}. The last variable involved in the calculation is the grain size d_ς transported by the cascade γ_ς under consideration, which determines also the typology of transport, and so which empirical sediment transport formulas need to be employed. As previously mentioned, two different empirical formulations, one for sand (*Engelund and Hansen*, 1967) and one for gravel (*Wong and Parker*, 2006), are available, quantifying in the two cases the dimensionless transport capacity $q_{S*e}{}^{\varsigma}$:

$$q_{S*e}{}^{\varsigma} = \begin{cases} \frac{0.05}{C_{fe}^{\varsigma}} \cdot \tau_{*e}{}^{\varsigma 5/2}, \text{if } d_\varsigma < 2 \times 10^{-3}\ m & (Engelund\ and\ Hansen) \\ \alpha \cdot (\tau_{*e}{}^{\varsigma} - \tau_{*ce})^{\beta}, \text{ else} & (Wong\ and\ Parker) \end{cases} \tag{2.6}$$

where

- C_{fe}^{ς} is the local friction factor

$$C_{fe}{}^{\varsigma} = \frac{2 \cdot g \cdot I_e \cdot h_e}{{v_e}^2}; \tag{2.7}$$

- $\tau*_e^{\varsigma}$ is the the dimensionless shear stress

$$\tau*_e{}^{\varsigma} = \frac{I_e \cdot h_e}{R \cdot d_\varsigma}; \tag{2.8}$$

- R is the relative density of sediment

$$R = \frac{\rho_S - \rho_W}{\rho_W}; \tag{2.9}$$

- $\rho_S = 2600\ kg\ m^{-3}$ is the sediment density and $\rho_W = 1000\ kg\ m^{-3}$ is water density;
- τ_{*ce} is the critical shear stress, assumed constant equal to 0.047 under fully turbulent flow conditions (*Wong and Parker*, 2006);
- parameters $\alpha = 3.97$ and $\beta = 1.5$ are derived from *Wong and Parker* (2006).

The dimensionless transport capacity ${q_{S*e}}^{\varsigma}$ obtained through equation (2.6) is then turned into the daily volumetric transport capacity ${q_{S,daily_e}}^{\varsigma}\ (m^2 d^{-1})$ per unit of channel width through

$${q_{S,daily_e}}^{\varsigma} = {q_{S*e}}^{\varsigma} \cdot 3600 \cdot 24 \cdot \sqrt{R \cdot g \cdot {d_{\varsigma}}^3}, \tag{2.10}$$

which is transferred in turn into a daily transport capacity in terms of $kg\ d^{-1}$ multiplying by the sediment density ρ_S and active channel width W_{ACe}:

$${Q_{S,daily_e}}^{\varsigma} = {q_{S,daily_{*e}}}^{\varsigma} \cdot \rho_S \cdot W_{ACe}. \tag{2.11}$$

Equations (2.6) - (2.11) are implemented through functions `Engelund_Hansen` and `Wong_Parker` according to the grain size class.

The transport capacity thus calculated is nevertheless an instantaneous value referred to specific hydraulic conditions, defined by a certain discharge Q_e determining hydraulics h_e and v_e used for the calculation of ${C_f}_e^{\varsigma}$ and ${\tau*}_e^{\varsigma}$ in equations (2.7) and (2.8). For the sake of the sediment fluxes simulation, transport capacities have to refer to standard hydrological conditions over a long time represented through local hydrographs $\boldsymbol{Q_e}$. Each hydrograph embodies information about magnitude and frequency of discharges in a certain reach e, determining the potential sediment entrainment which final ${Q_S}_e^{\varsigma}$ aims to quantify. The latter should then be obtained by combination of all capacity values corresponding to every daily discharge in the hydrograph, but as already mentioned this would be too much time-consuming: hence the synthetic representation of each hydrograph $\boldsymbol{Q_e}$ through mean discharges $Q_e(p)$ within percentile-defined classes p and classes' frequencies $n_e(p)$ introduced in the first part of this section. Therefore the final ${Q_S}_e^{\varsigma}$ is derived as weighted mean of just 8 transport capacities ${Q_S}_e^{\varsigma}(p)$ calculated for discharges $Q_e(p)$. Transport capacities ${Q_S}_e^{\varsigma}(p)$ are weighted by relative frequencies of related classes p and then multiplied by the total number of days in a year to obtain the final transport capacity in terms of $kg\ yr^{-1}$ according to

$${Q_S}_e^{\varsigma} = \frac{\sum_{k=1}^{p} {Q_{S,daily_e}}^{\varsigma}(k) \cdot n_e(k)}{n_{tote}} \cdot 365, \tag{2.12}$$

where $n_e(p)$ are the absolute frequencies of percentile-defined classes and n_{tote} is the length of the discharge time series available for reach e.

${Q_S}_e^{\varsigma}$ thus represents the maximum potential sediment transport of a generic cascade γ_{ς} through a generic reach e over an average year within the time horizon considered for the simulation.

Calculations discussed above are performed for each cascade in each reach of its pathway by function `CalculateQsij_par_func`, invoked in the second part of script `HydraulicCalcs`. Main inputs of the function are:

- cell array `stats`, including results of hydraulic calculations discussed in the previous section;
- matrices `Dmat` and `hydraulicData`, containing bankfull hydraulics and grain sizes d_ς calculated by the grain size solver in section 2.5;
- matrix `AggData` and structure `Network`, providing information about reaches in the river network.

The function loops through all rows of matrix `AggData`, i.e. all possible source reaches ς, and for each ς the list of downstream reaches composing the pathway κ_ς^Ω of cascade ς is identified based on the graph topology information contained in structure `Network`. For each ς a second level loop runs through all reaches $e \in \kappa_\varsigma^\Omega$, for each of which 8 (or less in case of duplicates) values of water level $h_e(p)$ and flow velocity $v_e(p)$ are available. Water levels $h_e(p)$ and flow velocities $v_e(p)$ are derived from mean discharges $Q_e(p)$ in percentile-defined classes p. Sediment transport formulas (2.6) - (2.11) implemented in functions `Engelund_Hansen` and `Wong_Parker` are then applied for each discharge $Q_e(p)$ in reach e. The functions therefore need to receive in input the following variables:

- the set of hydraulics $h_e(p)$ and $v_e(p)$ for each class p (stored in cell array `stats`);
- reach's morphology, consisting in slope I_e and active channel width W_{ACe} from matrix `AggData`;
- transported grain size d_ς from matrix `Dmat`.

The transport capacities $Q_{S,daily_e^\varsigma}(p)$ returned by functions `Engelund_Hansen` and `Wong_Parker` are then combined through weighted mean and turned into the final annual transport capacity $Q_{S_e^\varsigma}$ $(kg\ yr^{-1})$ as in equation (2.12), using as weights classes' relative frequencies derived from $n_e(p)$ and n_{tote} stored in cell array `stats`.

The above calculations are performed for every reach $e \in \kappa_\varsigma^\Omega$ from the source ς to the outlet Ω, unless one of the local transport capacities results to be zero (i.e. local hydromorphological conditions do not allow to entrain downstream the grain size d_ς). In this case the cascade is interrupted in that reach and the calculation of transport capacities is stopped, leaving all downstream reaches in the cascade pathway set to null value. Results for the current cascade γ_ς are stored in the ς^{th} row and in columns referring to reaches $e \in \kappa_\varsigma^\Omega$ of the output matrix `QS_s_e`.

The main loop runs through each cascade source, filling in matrix `QS_s_e` row-wise after calculating transport capacities cascade by cascade as described above.

In addition to matrix `QS_s_e` containing transport capacities $Q_{S_e^\varsigma}$, also the vector `QSin_s_0` of transport capacities $Q_{S_{e=\varsigma}^\varsigma}$ at cascade sources is provided , which will be used in the section 2.8 to define the initial supply Q_{S,in_ς} in the competition scenarios.

2.7 Competition scenarios

Transport capacities $Q_{S_e^\varsigma}$ calculated as described in the previous section would represent energy available for the transport of grain size d_ς through reach e if only cascade γ_ς were active in that reach. Generally multiple cascades cross the same reach though, so the energy of the river flow needs to be shared between all the locally active cascades. This idea is conceptually implemented in CASCADE model through competition: all active cascades in a reach e, denoted with Γ_e, "compete" with each other to get a share of the available energy. As a result of this operation a competition corrected transport capacity $Q_{S_e^{\varsigma\prime}}$ is assigned in every reach e to every cascade γ_ς.

High level assumptions are formulated about competition, originating 4 scenarios which vary in the calculation of the corrected transport capacities, but all provide for multiplying a dimensionless competition factor F_e^ς by a basic reference transport capacity $Q_{S_{ref}}$:

$$Q_{S_e^{\varsigma\prime}} = F_e^\varsigma \cdot Q_{S_{ref}}. \tag{2.13}$$

In scenarios 1 and 2, as reference transport capacity a measure of the locally available energy is used, that is the transport capacity $Q_{S_e}(d_{50e})$ calculated in reach e for the median grain size d_{50e} expected in that reach:

$$Q_{S_e^{\varsigma\prime}} = F_e^\varsigma \cdot Q_{S_e}(d_{50e}). \tag{2.14}$$

$Q_{S_e}(d_{50e})$ is computed and store in matrix `Qsd50` by script `calculateQsd50`, whose functioning is the same as for function `CalculateQsij_par_func` described in section 2.6, except for the grain size used. Functions `Engelund_Hansen` and `Wong_Parker` described in section 2.6 are indeed applied no more to the single grain size d_ς as in `CalculateQsij_par_func`, but to the median diameter d_{50e} representative of the ensemble of all the grain sizes transported through reach e by the cascades Γ_e. The grain size d_{50e} is calculated as the median of all the grain sizes transported by cascades originating upstream of reach e, so expected to cross e.[6]

Otherwise, scenarios 3 and 4 postulate that the corrected transport capacity is proportional to the initial supply $Q_{S,in}$ of the cascade γ_ς, rather then to the energy locally available in that reach, which on the other hand takes part in the calculation of the coefficient calculation F_e^ς:

$$Q_{S_e^{\varsigma\prime}} = F_e^\varsigma \cdot Q_{S,in_\varsigma}. \tag{2.15}$$

The initial sediment supply Q_{S,in_ς} at this stage is set equal to the transport capacity in the source reach:

$$Q_{S,in_\varsigma} = Q_{S_{e=\varsigma}{}^\varsigma} \tag{2.16}$$

calculated as described in the previous section by function `CalculateQsij_par_func` and stored in matrix `QSin_s_0`. Differently from scenarios 1 and 2, here there is no conservation of transport capacity since, even if all

[6] In fact the d_{50e} thus calculated at this point is just an approximation of the proper d_{50e}, which would require also information about the magnitude of cascade fluxes (yet to be simulated) in order to have a weighted median and to consider only active cascades (some of the upstream cascades may in fact be interrupted before due to transport capacity deficiency or exhaustion of the initial sediment load, as described later in section 2.8), so the actual d_{50e} can be estimated more precisely only at the end of the complete CASCADE simulation. However this approximation will not return a so different value than the weighted median resulting after the simulation of fluxes and it is necessary to avoid recursive calculations, which would make computational time rise.

the F_e^ς in reach e sum up to 1, the sum of all $Q_{S_e^\varsigma}'$ does not return the basic transport capacity, being Q_{S,in_ς} different for every cascade crossing reach e.

As regards competition factors, two different formulations are available. The first, implemented in scenarios 1,3 and 4 and named `F1` in the code, postulates that cascades with higher local transport capacity $Q_{S_e^\varsigma}$ get a higher share of the basic transport capacity $Q_{S_{ref}}$ through

$$F_e^\varsigma = \frac{Q_{S_e^\varsigma}}{\sum_{k\in\Gamma_e} Q_{S_e^k}}, \tag{2.17}$$

whereas a second possible formulation for F_e^ς, implemented in scenario 2 and named `F2` in the code, assumes that cascades with higher initial supply Q_{S,in_ς} are favoured in the competition:

$$F_e^\varsigma = \frac{Q_{S,in_\varsigma}}{\sum_{k\in\Gamma_e} Q_{S,in_k}}. \tag{2.18}$$

In the following the four competition scenarios are presented more in detail.

Scenario 1

Scenario 1, expressed by equation (2.19), postulates that cascades crossing reach e share the local transport capacity $Q_{S_e}(d_{50e})$ based on their own local transport capacity $Q_{S_e^\varsigma}$:

$$Q_{S_e^\varsigma}' = F_e^\varsigma \cdot Q_{S_e}(d_{50e}) \qquad \text{where} \quad F_e^\varsigma = \frac{Q_{S_e^\varsigma}}{\sum_{k\in\Gamma_e} Q_{S_e^k}} \tag{2.19}$$

therefore finer grain sizes are transported preferentially.

Scenario 2

Scenario 2, expressed by equation (2.20), postulates that cascades crossing reach e share the local transport capacity $Q_{S_e}(d_{50e})$ according to their initial supply Q_{S,in_ς}:

$$Q_{S_e^\varsigma}' = F_e^\varsigma \cdot Q_{S_e}(d_{50e}) \qquad \text{where} \quad F_e^\varsigma = \frac{Q_{S,in_\varsigma}}{\sum_{k\in\Gamma_e} Q_{S,in_k}} \tag{2.20}$$

so in this case high initial sediment supply cascades are favoured, rather than finer grain sizes.

Scenario 3

Scenario 3, expressed by equation (2.20), postulates that cascades crossing a certain reach e carry a greater share of the initial sediment supply Q_{S,in_ς} as higher their own local transport capacity $Q_{S_e^\varsigma}$ is:

$$Q_{S_e^\varsigma}' = F_e^\varsigma \cdot Q_{S,in_\varsigma} \qquad \text{where} \quad F_e^\varsigma = \frac{Q_{S_e^\varsigma}}{\sum_{k\in\Gamma_e} Q_{S_e^k}} \tag{2.21}$$

which means that for equal initial supply, cascades carrying finer grain size d_ς are favoured in the competition.

Scenario 4

Scenario 4 is analogous to scenario 3 as for the formulation of both the competition factor F_e^{ς} and the basic reference transport capacity $Q_{S_{ref}}$, but it assumes that competition only occurs between cascades carrying the same grain size class: sandy ($\leq 2\ mm$) or gravelly ($> 2\ mm$). This results in calculating the competition factor F_e^{ς} of a cascade γ_{ς} crossing reach e considering only the same grain size class cascades active in that reach:

$$Q_{S_e^{\varsigma}}' = F_e^{\varsigma} \cdot Q_{S,in_{\varsigma}} \quad \text{where} \quad F_e^{\varsigma} = \begin{cases} \dfrac{Q_{S_e^{\varsigma}}}{\sum_{k \in \Gamma_e|_{d_k \leq 2\times 10^{-3}\ m}} Q_{S_e^k}}, \text{if } d_{\varsigma} \leq 2 \times 10^{-3}\ m \\ \\ \dfrac{Q_{S_e^{\varsigma}}}{\sum_{k \in \Gamma_e|_{d_k > 2\times 10^{-3}\ m}} Q_{S_e^k}}, \text{if } d_{\varsigma} > 2 \times 10^{-3}\ m \end{cases} \tag{2.22}$$

This last formulation is based on the consideration that if both sand and gravel are transported along a river reach, the transport of sand does not interfere much with the transport of gravel. On the contrary, some studies have shown that the presence of sand might even increase the transport of gravel (e.g. *Wilcock and Crowe* (2003)) rather than reducing it as in scenario 3.

2.8 Cascade routing and simulation of sediment fluxes

Calculation of sediment fluxes, together with the competition calculations described in the previous sections, are performed sequentially cascade-by-cascade by function `CASCADE_Func`, which constitutes the core of CASCADE model and implements processes highlighted in the flow chart of figure 2.6. These basically consist in the calculation of corrected transport capacities (considering then competition between cascades crossing the same reach) and routing of each cascade, determining sediment fluxes and deposited fractions in every reach.

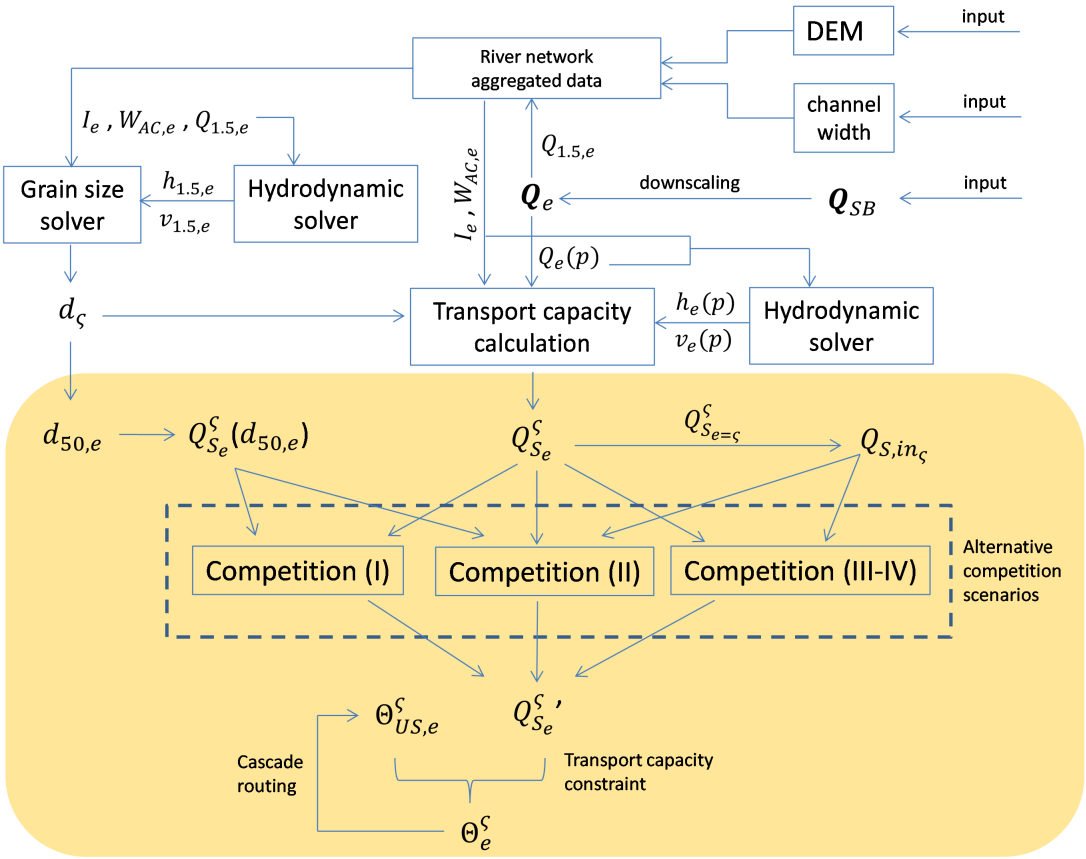

Figure 2.6: *Components and variables involved in the cascade routing phase and simulation of sediment fluxes described in section 2.8. Competition corrected transport capacities $Q_{S_e}^{\varsigma\prime}$ can be calculated according to 4 different scenarios. A reference transport capacity $Q_{S_e}(d_{50_e})$ (based on the median grain size d_{50_e} expected in each reach e) is involved in scenarios 1 and 2, whereas the initial supply Q_{S,in_ς} (set equal to the transport capacity value in the source reach $Q_{S_{e=\varsigma}}{}^{\varsigma}$) is used in scenarios 2,3 and 4. Finally, each cascade γ_ς is routed from the source ς to downstream through implementing reach-to-reach mass balances, where the sediment flux Θ_e^ς entrained through a reach e depends on the upstream incoming flux $\Theta_{US,e}^\varsigma$ and on the local corrected transport capacity $Q_{S_e}^{\varsigma\prime}$.*

Function `CASCADE_Func` routes sequentially all the cascades, implementing for each cascade γ_ς reach-to-reach mass balances from upstream to downstream along the pathway κ_ς in the graph, starting from the source reach ς (initialised with an initial supply of sediment Q_{S,in_ς}) up to the outlet Ω or until the cascade is interrupted. This may occur in three cases:

1. $Q_{S_e^{\varsigma\prime}} = 0$, i.e. the local corrected transport capacity is not sufficient to transport d_ς through reach e;
2. a dam is located in reach e (in case reservoirs are considered);
3. $\Theta_e{}^\varsigma < \phi_{thresh} \cdot Q_{S,in_\varsigma}$ (where ϕ_{thresh} is a percentage threshold), i.e. the cascade γ_ς initial load Q_{S,in_ς} has been almost totally exhausted by deposition during its routing between the source ς and reach e.

Cases 1 and 2 are related to local disconnectivity and can be evaluated before the simulation of sediment fluxes, allowing to perform calculations only for connected reaches, whereas case 3 is related to results of mass balances, so in this case disconnectivity information will be available only at the end of the routing of each cascade.

Focusing on the MATLAB implementation, function `createCascadeInputs` is used to group together all the inputs required by function `CASCADE_Func` into structure `CascadeInputs`, whose fields are:

- `AggData`: matrix containing raw graph information about the river network and channel widths (further details have been described in subsection 2.3.1);
- `hydraulicData`: matrix containing bankfull hydraulics and grain sizes d_ς calculated by the grain size solver in section 2.5;
- `Dmat`: matrix containing grain sizes d_e^ς delivered by cascade γ_ς through reach e, calculated by the grain size solver as dicussed in section 2.5;
- `stats`: cell array containing results of hydraulic calculations described in section 2.6;
- `Network`: structure containing information about the topology of the river network, obtained during the phase of graph preprocessing described in section 2.4;
- `II`: matrix containing topological distances between reaches (section 2.4);
- `outlet_node_new`: identification code of the outlet reach;
- `QSij`: matrix of transport capacities, obtained as described in section 2.6 as output of function `CalculateQsij_par_func` (at that stage called `QS_s_e`);
- `iswarmup`: boolean variable used to specify if the current run is the warming up (case 1) or not (case 0);
- `QSin_s_0`: vector of sediment supplies at sources Q_{S,in_ς} used for the competition scenarios, output of function `CalculateQsij_par_func` described in section 2.6;
- `Input_0`: same as `QSin_s_0`;
- `transport_threshold`: threshold ϕ_{thresh} for ratio $\frac{\Theta_e{}^\varsigma}{Q_{S,in_\varsigma}}$, defining the percentage of Q_{S,in_ς} under which a cascade is considered exhausted;
- `scenario`: string defining the competition scenario, which can be set to 'Scenario 1', 'Scenario 2', 'Scenario 3' or 'Scenario 4';

- `US_hierarchy`: vector containing the number of downstream reaches for every reach, obtained at the stage of graph processing described in subsection 2.4;

- `calculationOrderType`: string defining the sequential order in which cascades are routed, which can be set to 'upstream' (deafult option), 'downstream' or 'dod' (i.e. downstream of dams).

The warming up run allows to analyse sediment connectivity in an undisturbed state in absence of reservoirs and without any supply limitation. The warming up run can also be seen as the basis for further runs, considering instead the effect of dams or applying an upper bound for sediment supply (which however are not implemented in the code of the CASCADE version presented in detail in this work, nor have been applied in the case study presented in chapter 3). If a maximum sediment supply is to be imposed at cascade sources, an additional input is required in structure `CascadeInputs` to define the maximum limit for initial supply Q_{S,in_ς} for every cascade γ_ς, which may be set equal to lowest transport capacity $Q_{S_e^{\varsigma'}}$ along its pathway resulted from the warming up run. This operation can be performed by function `calculateQSin_s`, which returns the supply upper bounds and the bottle-neck reach for every cascade. Similarly, an additional run to consider the effect of reservoirs on the sediment connectivity requires providing appropriate inputs, to be included in structure `CascadeInputs`, defining their locations in the river network.

Input `calculationOrderType` defines the order in which cascades are routed. The order of routing can be defined based on the topological position of their reach sources ς: if string 'upstream' is entered, cascade sources are sorted in vector `calculation_order` from upstream to downstream according to the descending number of downstream reaches (contained in vector `US_hierarchy`), so that cascades starting from upstream are routed first. On the contrary if `calculationOrderType` is set to 'downstream', then cascade sources are sorted from downstream to upstream according to the ascending number of downstream reaches so that cascades originating from downstream sources are routed first. In case reservoirs are present and modelled in the river network, it might be preferable to route first cascades starting downstream of dams: hence the third option encoded by string 'dod'.

Function `CASCADE_Func` loops through all the cascade sources stored in vector `calculation_order` in order to route a cascade at a time.

At first the expected pathway κ_ς^Ω of the current cascade γ_ς, composed by all reaches downstream of the source ς up to the river network outlet Ω, is derived from topological information contained in `Network` structure. Hence the actual pathway κ_ς is obtained by cutting off disconnected reaches downstream of any interruption due to local disconnectivity issues (i.e. null local transport capacity or the presence of a dam, if reservoirs are modelled). After that κ_ς is stored in temporary variable `ds_path_nodes` and information about disconnected reaches is stored in matrix `Discon_for_local`. Corrected transport capacities $Q_{S_e^{\varsigma'}}$ are then calculated only for connected reaches $e \in \kappa_\varsigma$, saving computational time.

Competition calculations depend on the chosen scenario, as described in the previous section on a conceptual level. $Q_{S_e^{\varsigma'}}$ are derived through one of equations (2.19), (2.20), (2.21) and (2.22) based on:

- transport capacities $Q_{S_e}^{\varsigma}$ stored in matrix `TranspC_mat1` (as input matrix `QSij` is renamed within the function `CASCADE_Func`);
- initial supplies Q_{S,in_ς}, stored in input vectors `QSin_s_0` and `Input_0` equivalently;
- local $Q_{S_e}(d_{50e})$, calculated by script `calculateQsd50` invoked within function `CASCADE_Func` and stored in matrix `Qsd50`.

In terms of MATLAB variables, elements of matrix `TranspC_mat2` belonging to the ς^{th} row and columns defined by vector `ds_path_nodes` are filled in with calculated transport capacities $Q_{S_e}^{\varsigma\prime}$.

Once the calculation of corrected transport capacities for the current cascade is achieved, next step is calculating sediment fluxes for the current cascade along the pathway κ_ς from the reach source ς up to the outlet or any eventual interruptions.

Every sediment flux Θ_e^{ς} of cascade γ_ς crossing reach e is computed through a reach-to-reach mass balance illustrated by equation (2.23). The input sediment flux $\Theta_{US,e}^{\varsigma}$ coming from upstream is completely delivered trough the current reach e only if the local corrected transport capacity $Q_{S_e}^{\varsigma\prime}$ is sufficient (case 1), otherwise only a share equal to $Q_{S_e}^{\varsigma\prime}$ can be routed (case 2), while the excess is deposited in reach e:

$$\Theta_e{}^{\varsigma} = \begin{cases} \Theta_{US,e}^{\varsigma} \text{ if } \Theta_{US,e}^{\varsigma} < Q_{S_e}^{\varsigma\prime} & \text{(case 1)}, \\ Q_{S_e}^{\varsigma\prime} \text{ else} & \text{(case 2)}. \end{cases} \tag{2.23}$$

The mass balance illustrated by equation (2.23) is performed reach per reach proceeding downstream along the cascade pathway κ_ς starting from the second reach of κ_ς. For the first reach in the cascade pathway, i.e. the source reach $e = \varsigma$, no upstream flux $\Theta_{US,e}^{\varsigma}$ is defined, so the sediment flux Θ_e^{ς} crossing the source reach needs to be initialised *a-priori* to the initial supply Q_{S,in_ς}. The latter represents the sediment flux due to detachment in the source reach ς supplying the cascade source γ_ς and it is set equal to the corrected transport capacity in the source reach $e = \varsigma$ according to equation

$$Q_{S,in_\varsigma} = Q_{S_{e=\varsigma}}{}^{\varsigma\prime} \tag{2.24}$$

along the lines of what done for the Q_{S,in_ς} used to derive the corrected transport capacities in scenario 2,3 and 4 as described in section 2.7 (equation (2.16)).[7]

Following downstream fluxes are calculated according to equation (2.23) up to the outlet or till the cascade γ_ς is interrupted (i.e. $\Theta_e{}^{\varsigma} = 0$), which may occur for local disconnectivity or by exhaustion of the initial sediment load of the cascade, as discussed at the beginning of section 2.8. Local disconnectivity issues, as already mentioned, allow to limit the calculation of corrected transport capacities and sediment fluxes to the pathway that κ_ς stored in temporary variable `ds_path_nodes`, deprived of disconnected reaches listed in matrix `Discon_for_local`. Still cascade γ_ς may be interrupted before the end of the pathway identified by `ds_path_nodes` in case the initial load

[7] At that stage transport capacity $Q_{S_{e=\varsigma}}{}^{\varsigma}$ was used instead of $Q_{S_{e=\varsigma}}{}^{\varsigma\prime}$ yet to be calculated, so it must paid attention not to confuse the two quantities both denoted with Q_{S,in_ς}, but calculated at different stages from different available information.

Q_{S,in_ς} has been almost totally exhausted by deposition. This last kind of disconnectivity is not due to local reach's conditions, but results from the simulation of sediment fluxes by mass balance according to

$$\Theta_e{}^\varsigma = 0 \qquad \text{if} \quad \Theta_e{}^\varsigma < \phi_{thresh} \cdot Q_{S,in_\varsigma} \tag{2.25}$$

where ϕ_{thresh} is a percentage threshold for the minimum flux with respect to the initial supply. For instance, if ϕ_{thresh} is set to 0.05, the cascade is considered interrupted in a certain reach e if the 95% of the initial supply Q_{S,in_ς} has been deposited during its pathway between the source ς and reach e.

If cascade γ_ς is thus interrupted, the routing stops and reaches $\boldsymbol{disc_{MB}}$ downstream of e belonging to κ_ς are disconnected because of exhaustion of the initial sediment load resulted from simulated mass balances. In these reaches γ_ς is not active any more, so it will not take part in competition with other cascades yet to be routed. To consider this, transport capacities $Q_S{}^\varsigma{}_{\boldsymbol{disc_{MB}}}$ and $Q_S{}^{\varsigma\prime}{}_{\boldsymbol{disc_{MB}}}$ corresponding to these reaches need to be deleted from matrices `TranspC_mat1` and `TranspC_mat2` in the ς^{th} row referred to cascade γ_ς. Information about disconnected reaches $\boldsymbol{disc_{MB}}$ is then stored in matrix `Discon_for_mbal`. It shall be considered that the calculation of corrected transport capacities and sediment fluxes is not recursive, so previously routed cascades are not updated considering interruptions resulting from the simulation fluxes: cascades yet to be routed then may have been improperly considered in competition calculations in reaches in which they will not result to be actually active. On the other hand this may favour cascades calculated in the end, for which CASCADE is able to take into account also this kind of interruptions for previously calculated cascades. Therefore the calculation order can affect results of the simulation.

Once a cascade has been completely routed, the corresponding row in matrices `Input` and `Output` is respectively filled with $\Theta^\varsigma_{US,e}$ and Θ^ς_e values referred to every reach e belonging to the pathway of γ_ς.

After all cascades have been routed, the function returns as output variables the matrices `Input` and `Output`, containing incoming $\Theta^\varsigma_{US,e}$ and outgoing Θ^ς_e fluxes, as well as matrix `TranspC_mat2` containing final corrected transport capacities $Q_{S_e}{}^{\varsigma\prime}$.

CHAPTER 3

Piedmont case study

3.1 Geographical framework

The Piedmont Region is located in the North West of Italy and it is entirely included in the upper part of the basin of the Po River, which rises in Piedmont from the Monviso, in the Western Alps, and crosses the whole region from west to east.

The region is surrounded on three sides by mountains: the Alps separate Piedmont from France at the western boundary and from Switzerland and the Italian region of Aosta Valley at the northern boundary, whereas Apennines border the region with the Liguria Region. The central part of the region is occupied by the Padan Plain north of the Po River and by the hill areas of the Langhe and Montferrat south of the stream. In the East Piedmont borders Lombardy and Emilia Romagna regions.

43.3% of the territory is mountainous, 30.3% is hillside and the remaining 26.4% is occupied by the Padan Plain. Most of the mountains belong to the chain of the Alps, whose higher peaks are higher than 4000 metres, whereas Apennines in the south of the region do not reach the altitude of 2000 metres above sea level.

The Piedmont Region is characterised by temperate climate, with most precipitation in spring and autumn in the plain, whereas in the mountains there is alpine climate. The melting of snow and glaciers in the Alps supplies rivers also during the warm season, when in the plain precipitations are less frequent, whereas rivers rising from the Apennines are characterised by torrential stream.

Most of Piedmont rivers transport gravelly sediment loads and several were subject to severe river channel alterations (i.e. narrowing, river bed incision, etc.) during the last century due to various types of human disturbance (*Surian and Rinaldi*, 2003).

3.1.1 Hydrographic network under study

The river network under study belongs to the upper Po basin closed just downstream of the confluence with the Scrivia River, almost totally included in the Piedmont Region. Figure 3.1 shows rivers composing the hydrographic network considered for the simulation.

The Po River is the main Italian river, crossing Northern Italy from its source in the Western Alps to the mouth into the Adriatic Sea in the North East of Italy. The left-bank side is located north of the Po stream and, as regards the basin under consideration, is crossed by the Po tributaries Sesia, Dora Baltea, Orco, Stura di Lanzo, Dora Riparia and Pellice. Main right-bank tributaries located in the southern part of the region are Tanaro, Bormida and Scrivia. Other rivers considered in the simulation are the Sessera

Figure 3.1: *Hydrography of Piedmont region: main rivers composing the river network considered for the present case study*

(a tributary of the Sesia), the Stura di Demonte (a tributary of the Tanaro) and the Gesso (a tributary of the Stura di Demonte). As regards the Bormida River, the upper stretch is known as Bormida di Millesimo upstream of the confluence with its tributary Bormida di Spigno. Several small reservoirs are present in the basin considered for the simulation, which however does not include the bigger lakes of the region, i.e. Lake Maggiore and Lake Orta (belonging to the basin of the Ticino River, which joins the Po in Lombardy downstream of the outlet).

3.2 Data preparation

The aim of the work described in this section is to provide input variables for CASCADE simulation, listed and described in detail in section 2.3, exploiting at best all available data. In particular high-quality channel width data are provided by a river classification work (carried out by *Demarchi et al.* (accepted) and roughly described in section 3.2.3) for the river network displayed in figure 3.1, including only main rivers within Piedmont Region's borders. This constitutes an important novelty because it is the first time that CASCADE is applied with so detailed morphological information. Subsection 3.2.1 will be dedicated to describe how the river network graph has been obtained in order to fit at best the river network for which channel width data are available.

3.2.1 River network

The river network displayed in figure 3.1, for which channel width data are available, needs to be modelled through a graph composed by nodes and edges, implemented in MATLAB through matrix `AggData` described in section 2.3.1. This were obtained in several steps, involving MATLAB coding and the use of a GIS software, based on a Digital Elevation Model (DEM).

Digital Elevation Model

The digital elevation model used was provided also from the work of *Demarchi et al.* (accepted): it is derived from a LIDAR DEM at 5 metres ground resolution, obtained through a flight acquisition campaign commissioned by the Piedmont Region during the years 2009/2010. LIDAR imageries were then projected into the Lambert azimuthal equal-area projection (LAEA) according to the INSPIRE Directive by the European Commission (2007).

For the network extraction a down-sampled version of the DEM was used, in order to smooth the DEM and avoid problems due to any discontinuities for the generation of the river network, so that final ground resolution is 25 metres.

The DEM covers only the territory included within the administrative boundary of the Piedmont Region, implying some difficulties for the extraction of the river network. The Scrivia confluence, and so the outlet of river network to be modelled, is indeed located in Lombardy few kilometres outside the regional border, so a small portion of the Lombardy DEM (downloaded from the Lombardy Geo-portal) had to be integrated through the use of a GIS software. This operation allowed MATLAB function `ExtractRiverNetwork` (to be described in the following) to recognise the con-

fluence and so consider also the Scrivia basin in the identification of Piedmont river network.

Extracting the river network

Script `Script_River_Network_Piemonte` and function `ExtractRiverNetwork` were developed in the context of this thesis work to derive the graph for the river network from digital elevation data. Within function `ExtractRiverNetwork` key steps for the processing of the DEM are performed by functions provided by *Topotoolbox*. Topotoolbox is a MATLAB toolbox developed by *Schwanghart and Kuhn* (2010) providing a set of functions for topographic analysis. In detail, for this work the second version of Topotoolbox (*Schwanghart and Scherler*, 2014) was used.

User-defined parameters need to be specified within `Script_River_Network_Piemonte` and consist in the standard length of reaches and the drainage area threshold, which is the minimum drainage area for a cell to be recognised as part of the stream network. Low values of the threshold lead to very complex and detailed networks, whereas high values allow to identify only main streams. The script transfers user-defined parameters into settings for function `ExtractRiverNetwork`, receiving in input also the DEM. Then Topotoolbox functions enable to preprocess the DEM by filling sinks, calculate flow directions and hence the accumulation matrix, whose elements contain the number of upslope cells and can be turned into drainage areas multiplying by the area in km^2 of each cell. Flow directions and drainage areas not inferior to the specified threshold are then used to derive the stream networks present over the territory covered by the DEM, among which only the main one is maintained. The stream network is then dissected into reaches and an identifier is assigned to each. Reaches are then organised row-wise in a structure called `MS`, whose fields are filled with main properties of every reach calculated by the function, consisting in:

- geometry features, including vectors of points' coordinates;
- reach identifier;
- identifier of upstream and downstream node;
- elevation of upstream and downstream node;
- length;
- mean slope;
- Strahler order;
- drainage area (conventionally referred to the upstream node);
- coordinates of upstream and downstream node.

Scalar attributes are then converted into a matrix called `attributes`, which after the addition of a field for active channel width will be renamed as `Aggdata` (i.e. the matrix containing all basic river network information required by CASCADE, described in section 2.3.1). Function `ExtractRiverNetwork` returns matrix `attributes` and structure `MS`, where the latter is used to create a shapefile of the river network. In addition the matrix `nodes` is returned, containing the following fields:

1. node identifier;

2. X coordinate (m);
3. Y coordinate (m);
4. elevation ($m\ a.s.l.$);
5. drainage area (km^2).

Fitting the river network to available data

As described in the previous paragraph, the river network is automatically extracted from the DEM and the only way to control the selection of the various rivers consists in setting a proper threshold area. Nevertheless the aim of this phase was to identify a specific river network, displayed in figure 3.1, for which channel width data are available. As evident from the picture, the Scrivia stream is identified with a higher level of detail than other rivers. Moreover some relatively relevant rivers are neglected, so whatever drainage area threshold will not return the desired river network.

To face this problem two different river networks were extracted from the same DEM, one with high level of detail (threshold set to 3 km^2) and one more basic (threshold set to 50 km^2). For both networks the shapefile was created and imported to GIS environment, where all reaches non-matching with the rivers provided with width data were deleted. Only the Scrivia river network was maintained from the first shapefile and the rest of Piedmont river network was maintained from the second shapefile.

At this stage two river networks matching width data were available then: to merge them into the desired network script `Script_merge_river_networks` was used, in which identifiers of nodes and reaches are reassigned in order to match the identifier of the outlet node of the Scrivia river network with the identifier of the corresponding confluence node in the river network of the rest of Piedmont. New outputs matrices `attributes` and `nodes` and a new shapefile were then created for the final river network.

3.2.2 Drainage area correction

As mentioned in section 3.2.1, the digital elevation model used for this work includes only the Piedmont Region within its administrative borders, which do not everywhere correspond to watersheds. The most evident cases are at the borders with the Aosta Valley Region, which is entirely included within the Po basin, and at the southern boundary with the Liguria Region, where some left-bank tributaries of the Po River have their sources and non-negligible portions of their basins. In detail, rivers involved are:

1. Dora Baltea (with 3261 km^2 of basin in Aosta Valley);
2. Bormida di Spigno (about 310 km^2 in Liguria);
3. Bormida di Millesimo (about 240 km^2 in Liguria);
4. Scrivia (about 300 km^2 in Liguria).

This issue leads to an underestimation of drainage area for most reaches, being it calculated automatically by function `ExtractRiverNetwork` from the digital elevation model as described in section 3.2.1. This underestimation may cause serious problems since many calculations such as morphological and hydrological regressions are based on drainage area. To fix this problem `Script_adjust_drainage_area`, invoked in the preprocessing section of `Main_script_CASCADE_Piemonte`, was developed: the missing drainage areas listed above are added for all reaches downstream of the unrecognised external basins.

3.2.3 Active channel width

Raw data used to derive active channel width of every reach are provided by the results of a classification carried out by *Demarchi et al.* (accepted) for the concerned river network, using a procedure previously applied to the only Orco River (*Demarchi et al.*, 2016). The procedure consists in a semi-automated classification of essential geomorphic features based on near-infrared imagery (VHR) and LIDAR topography, comprising two main steps:

- Step 1: machine learning classification of riverscape units;
- Step 2: expert-based post classification.

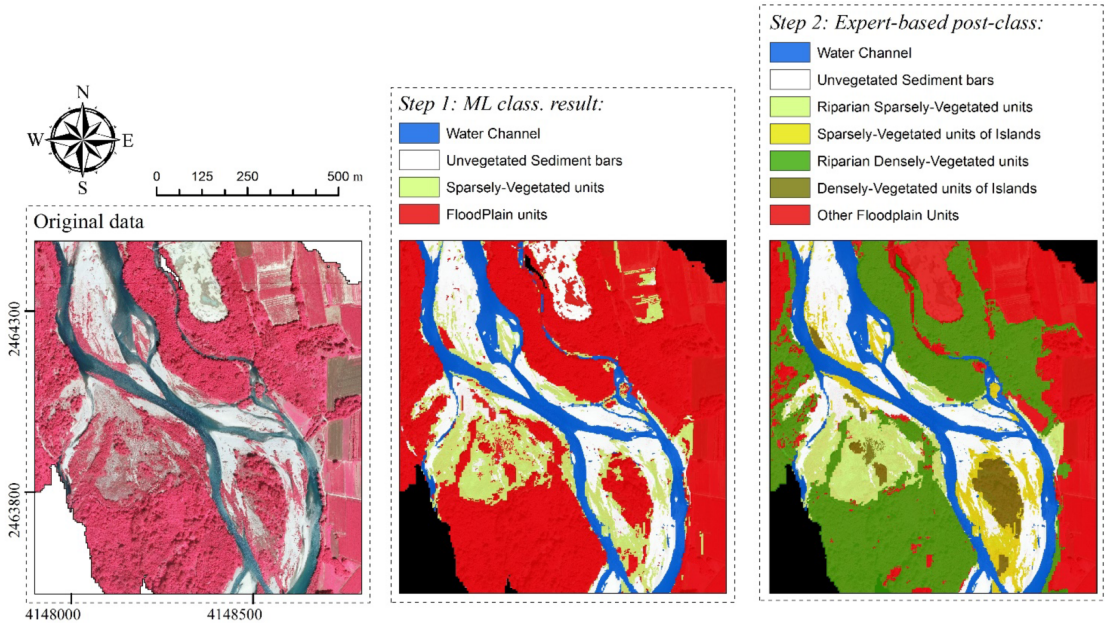

Figure 3.2: *Example of results of the riverscape units classification: Step 1 obtained with machine learning classification and Step 2 improvements after expert-based post-processing. (figure edited from Demarchi et al. (2016))*

The process results in the segmentation of areas and the classification into the following river riverscape units, as visible in figure 3.2:

- water channel;
- unvegetated sediment bars;

- riparian sparsely-vegetated units;
- sparsely-vegetated units of islands;
- riparian densely-vegetated units;
- densely-vegetated units of islands;
- other floodplain units.

Figure 3.3 shows some examples from the results of the approach extended to the regional scale.

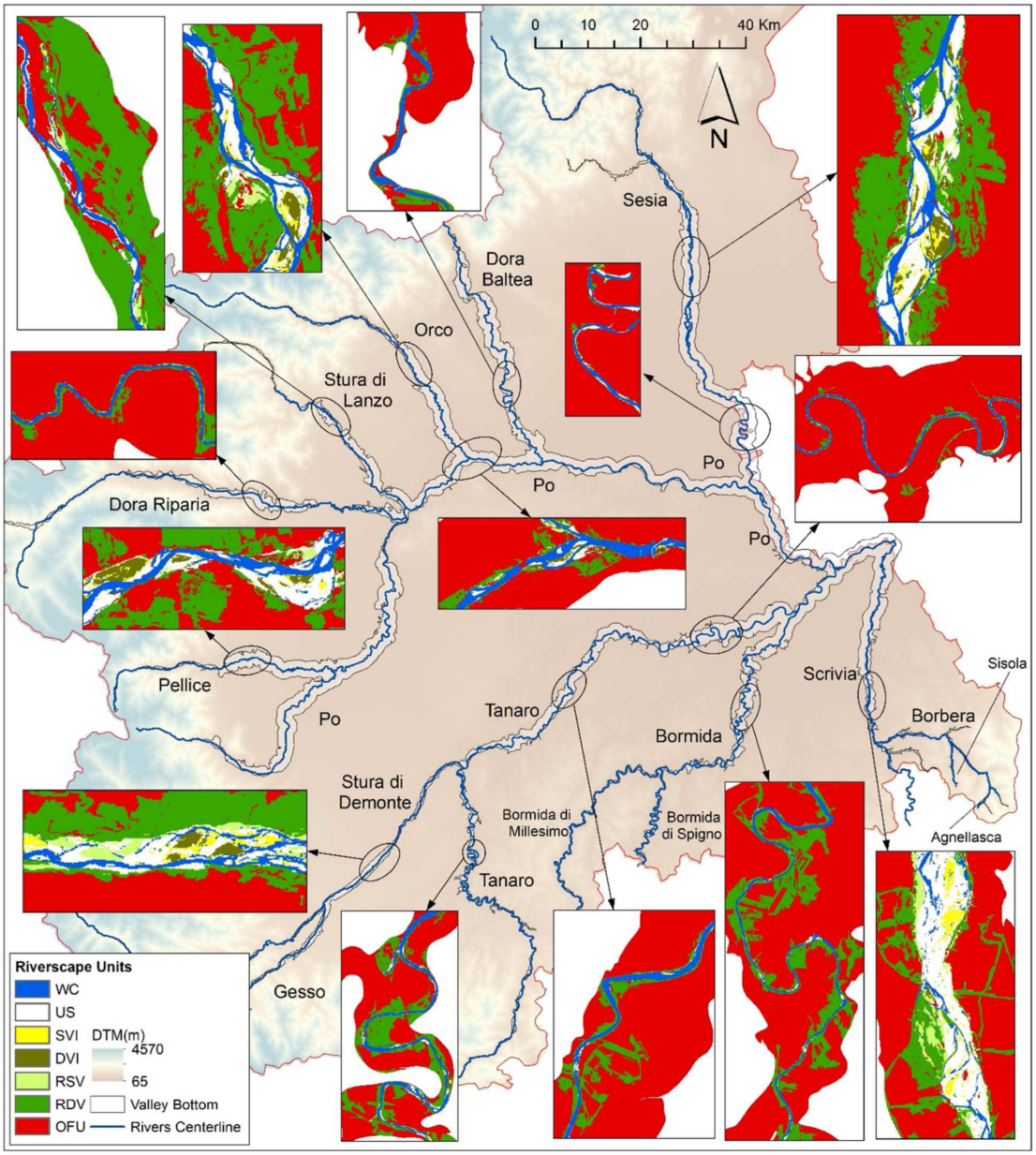

Figure 3.3: *Riverscape units for a set of reaches at the regional scale (figure edited from Demarchi et al. (accepted)).*

Resulting data are in form of a shapefile, disaggregated into spatial units called Disaggregated Geographical Objects (DGO) measuring 100 metres each. For each DGO

area measurements for each landscape unit are available, so width estimates were derived by dividing areas corresponding to active channel width by 100 metres. In detail, areas classified as water channel and unvegetated sediment bar were used for the grain size initialisation (see section 2.5) under bankfull conditions, while for the actual sediment fluxes simulations only water channel area were selected. The channel section is indeed assumed rectangular in CASCADE calculations, so a wider section is used to simulate bankfull conditions postulating that also the unvegetated sediment bar is flooded, whereas under average conditions only the main channel is assumed to be active.

Once channel widths are calculated for every DGO, measurements need to be derived for reaches in the river network obtained as described in section 3.2.1. Firstly DGOs were associated to corresponding reaches of the river network by performing an intersection between the two shapefiles in GIS environment, then the width in each reach was calculated as mean of non-void widths of all DGOs assigned to that reach.

Finally, derived widths can be used to calibrate a power-law regression on drainage area to estimate width for reaches in which no data are available or to use interpolated values instead of originals. In this exercise original values, characterised by higher heterogeneity, were maintained for the grain size initialisation to better reproduce natural variability, but for the rest of the simulation interpolated values were instead used to avoid problems due to discontinuities between consecutive reaches in simulating continuous processes such as river flow and sediment delivery. The operations just described are performed by `Script_wac`, invoked in the preprocessing section of main script `Main_script_CASCADE_Piemonte`.

3.2.4 Hydrology

Time series of daily discharges were downloaded from the hydrological database of ARPA Piemonte for 32 gauging station spread over the Piedmont river network (displayed in figure 3.4 in the following section). The time horizon chosen is 11 years long, from $1/1/2004$ to $31/12/2014$. Raw data were organised as described in section 2.3.2 and transferred into the MATLAB table `hydrologicData`.

3.3 Preprocessing

3.3.1 Hydrology

`Script_gauging_ stations`, invoked in the section `Process hydrologic data` of main script `Main_script_CASCADE_Piemonte`, associates each gauging station SB, in which an observed hydrograph is available, to the closest node e_{SB} of the river network. To associate the right node to each station the script identifies all nodes within a certain radius (herein set to 3 km) around the station and selects the one with the most similar drainage. Results of the automatic research have been double checked afterwards by graphical validation. The output variables of this phase are stored in matrix `RefLocations`, containing identifiers, geographical coordinates and drainage area of gauging stations and related nodes in the graph representing the river network.

Selected gauging stations are then associated to reaches having as upstream node the nodes selected by `Script gauging stations`: every reach e is assigned the

closest reference gauging station within the same sub-basin SB_e, that is the next gauging station downstream of e. Figure 3.4 shows the result of the assignment.

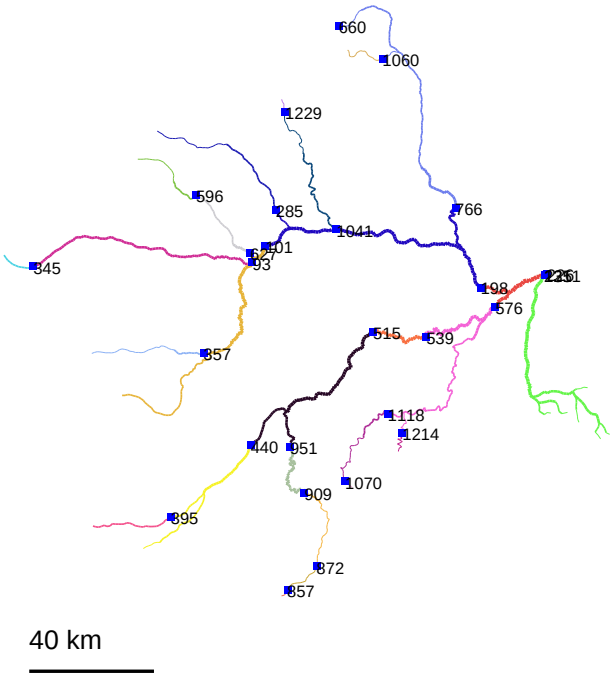

Figure 3.4: *Reference gauging stations of reaches: every reach of the river network is assigned the first downstream station. Reaches plotted in the same colour are assigned the same reference gauging station. Blue dots show the positions of gauging stations in the network, identified by the displayed reach identifier.*

Observed hydrographs corresponding to selected gauging stations are then imported and grouped into MATLAB table `hydrologicData`. From raw observed hydrographs 1.5 year discharges $Q_{1.5SB}$ are derived. The power law regression

$$Q_{1.5SB} = a * A^b_{D_{SB}} \tag{3.1}$$

mentioned in section 2.4 is then performed, resulting a very high R^2 as displayed in figure 3.5.

3.4 Grain size initialisation

In absence of field observations for the whole river network, grain size of cascades have been initialised with results of hydraulic calculations described in 2.5. This represents for sure a limitation because real data would guarantee a better accuracy, still it provides an acceptable approximation necessary to proceed. As discussed in section 3.2.3, original widths derived from areas classified as water channel and unvegetated sediment bar were used to reproduce bankfull conditions.

Numerical results will be discussed in section 4.3.

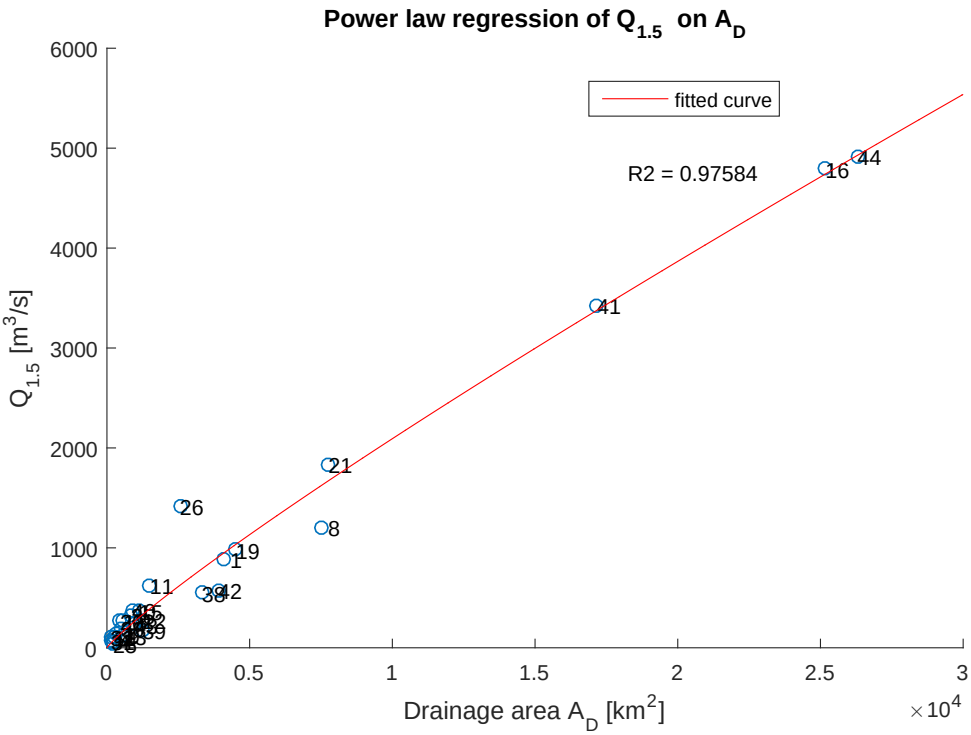

Figure 3.5: *Regression of the 1.5 year discharge $Q_{1.5}$ on drainage area A_{De}: calibration of the power law using gauging stations data*

3.5 Running CASCADE

The simulation carried out for the Piedmont river network was performed through the warming up run of function `CASCADE_Func`, in order to analyse potential sediment connectivity in an undisturbed state in absence of reservoirs and without any supply limitation.

As previously mentioned, whereas the grain size initialisation was performed by using originally calculated widths, for the calculations of transport capacities and for the cascade routing interpolated values on drainage areas were instead used, which gradually increase with the drainage area to avoid problems of discontinuity between reaches. Similarly, also slopes calculated based on the DEM elevations were interpolated through a power-law regression on drainage area to avoid such issues. Moreover slopes extracted from the DEM were derived from the elevations of the river bed rather then those of the water level, which are supposed to vary more gradually, like interpolated values do. The attribute matrix `AggData` was thus updated substituting interpolated widths and slopes for original values.

As for user-defined settings:

- the threshold ϕ_{thresh} was set to 10^{-4};
- as input `calculationOrderType`, string 'upstream' was entered;
- as input `scenario`, string 'Scenario 4' was entered.

As discussed in section 2.8 on page 29), the calculation order may affect results of the simulation. If indeed local disconnectivity can be evaluated before the simulation

of sediment fluxes, disconnectivity due to results of mass balances is only available at the end of the routing for each cascade. This results in considering in calculations for a generic corrected transport capacity $Q_{Se}^{\varsigma\prime}$ in a reach e also other cascades rising in source reaches downstream of ς (so yet to be routed), which however may result after the complete simulation to be not active in reach e because stopped upstream of e due to exhaustion of the initial sediment load Q_{S,in_ς}. Based on this consideration the option 'upstream' seemed to be the most convenient. Since cascades starting from upstream are more likely to be interrupted by exhaustion before reaching the outlet (being longer the pathway in which deposition can reduce the initial sediment load), routing them first allows to take into account these interruptions during subsequent routing of downstream cascades.

With respect to the competition calculations described in section 2.7, scenario 4 was chosen as it represents an upgrade of scenario 3, which had provided good results for the Da River case study (*Schmitt et al.*, 2016).

Results of the simulation of sediment fluxes and related elaborations are presented in chapter 4.

CHAPTER 4

Results

In this section results of CASCADE run for the Piedmont case study are presented, to both show the potentiality of CASCADE model and validate it through the comparison with field observations and results from previous studies. Results have to be looked at in terms of potential connectivity, not being considered the effect of reservoirs and supply limitation at sources in the simulation.

4.1 Grain size simulation

Through the elaboration of CASCADE outputs, in particular of sediment fluxes and grain sizes delivered by cascades, it is possible to derive an estimate of the median grain size d_{50} of sediments passing trough a reach. The distribution of sediments in every reach is conceptually due to active crossing cascades, where every cascade γ_ς carry its own grain size d_ς according to the initialisation at the source ς. The grain size d_ς of each cascade γ_ς is then weighted by the flux Θ_e^ς to obtain the local distribution in reach e, from which the 50% percentile d_{50e} is extracted in order to have a single representative element to be plotted in a synthetic picture. Figure 4.1(b) shows the result of this operation: median grain sizes resulting from CASCADE simulation are plotted for every reach. The pattern emerging from the figure is an overall fining of the median transported grain size in downstream direction, as generally observed in rivers. This result is a direct consequence of the entraining of the initialisation grain sizes shown in 4.1(a), where upstream sources have coarser sediments. Therefore downstream cascades, carrying finer sediments, are generally favoured in the competition with upstream cascades. The implemented competition scenario (i.e. scenario 4 described in section 2.7) postulates indeed that cascades with finer grain size, for equal initial supply, are more competitive (i.e. are able to deliver a higher fraction of the

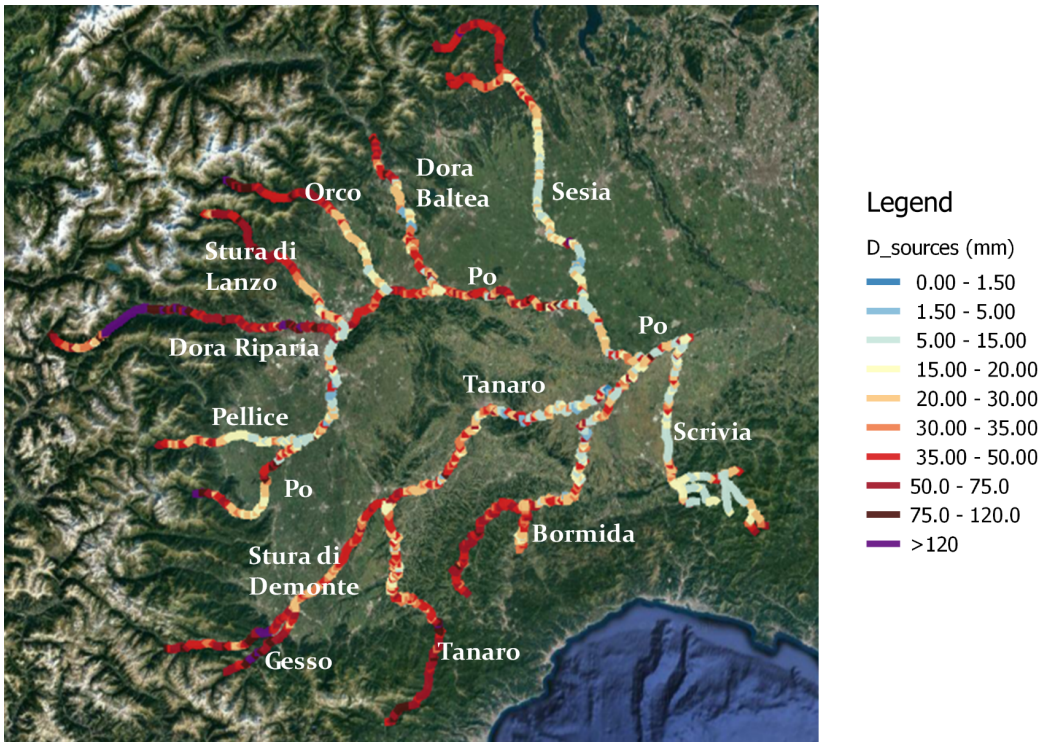

(a) Grain size initialisation at cascades sources $[mm]$.

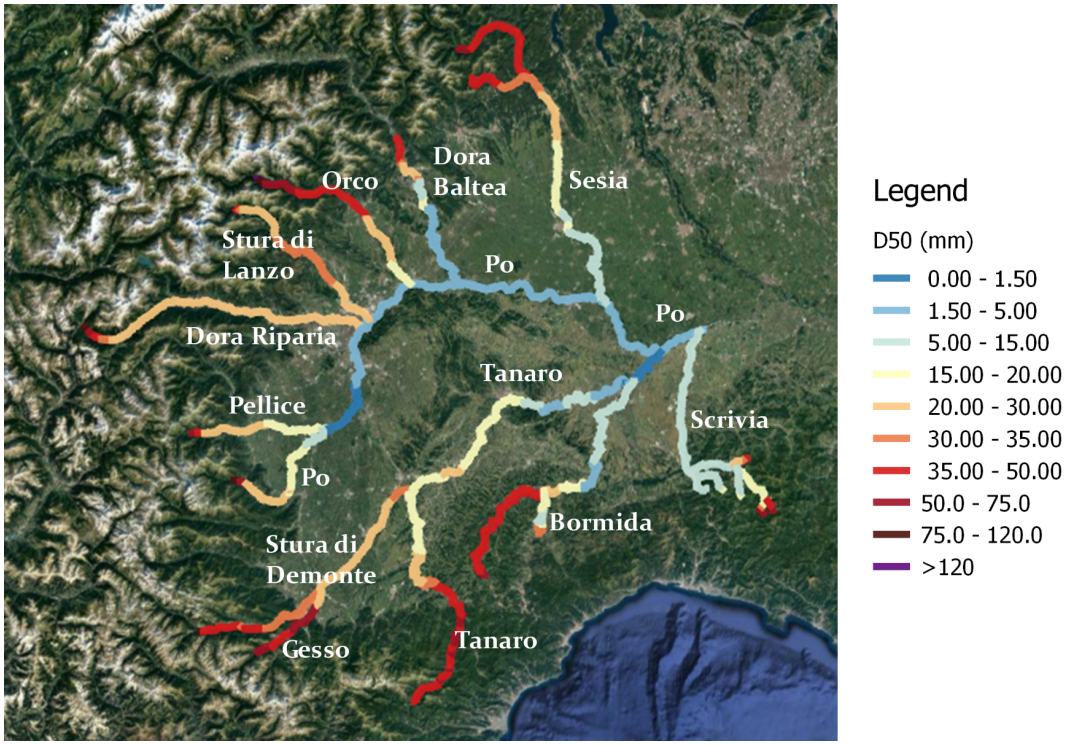

(b) Median grain size (d_{50}) simulated over reaches $[mm]$.

Figure 4.1: *Grain size initialisation and simulation over the river network*

initial sediment load). This is even more true in case of sandy cascades, whose transport capacities are not reduced at all by competition with other cascades, which carry gravelly sediment loads. Moreover cascades delivering coarser sediments, generally coming from sources located in upstream reaches of the network, are more likely to stop before other cascades because they require higher energy, and so higher slopes, to entrain sediments. Therefore interpolated slopes decreasing downstream with the increase of drainage area could become insufficient at a certain point. If original slopes were used, these cascades would suffer from bottleneck reaches with particularly low slope.

4.2 Delivery to the outlet

Another interesting feature of CASCADE is keeping track of source-sink relationships: this constitutes an innovation in the domain of sediment connectivity models, for previous models could not provide information about the provenance, but only about the magnitude of sediment flux in a river section. This property allowed to calculate the contribution of every source reach to the outlet sediment flux, plotted in figure 4.2.

The final delivery $\Theta^{\varsigma}_{\Omega}$ of each cascade γ_{ς} is only a share of the initial load $Q_{S,in_{\varsigma}}$ (set equal to the corrected transport capacity at the source according to equation (2.24)), reduced by the amount of sediment deposited along the cascade path because of competition with other cascades. In figure 4.2 this kind of contribution is displayed for every source reach. Most reaches reveal to be potentially connected to the outlet, also those rising very upstream in the basin. Greatest fluxes arrive from rivers located near the

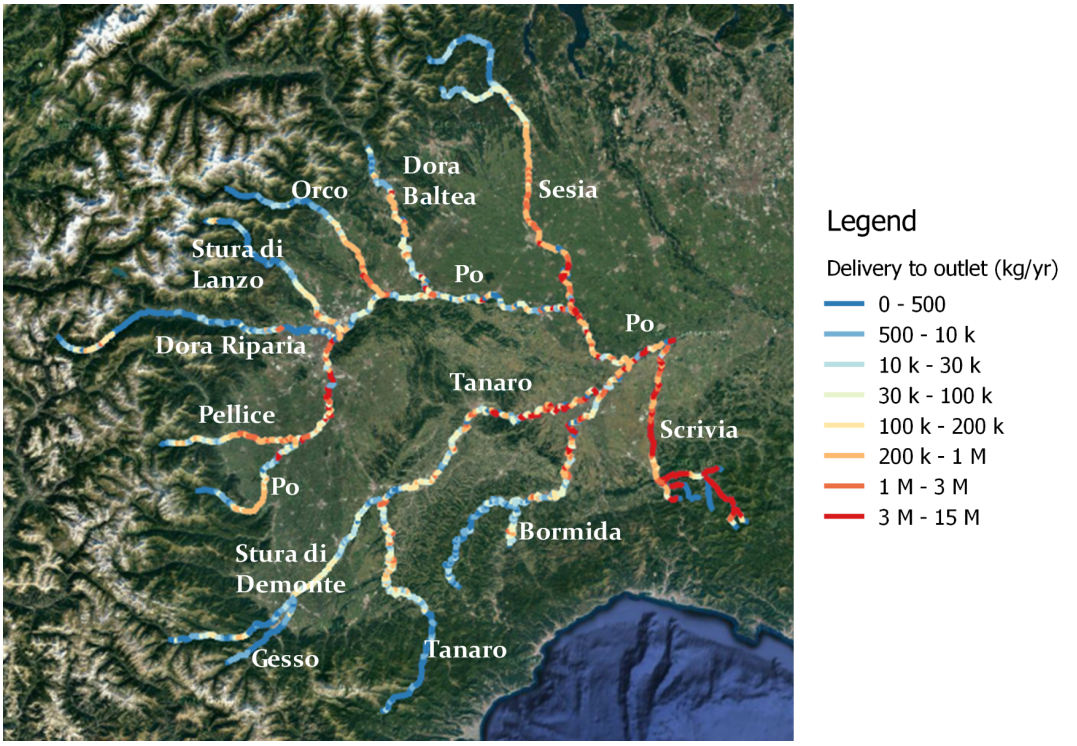

Figure 4.2: *Delivery to the outlet: the value assigned to each reach ς represents the amount of sediment $\Theta^{\varsigma}_{\Omega}$ that a cascade originating in source ς achieves to deliver up to the outlet Ω in terms of kg/yr*

outlet, such as the Scrivia and the downstream stretch of Sesia, Tanaro, and Bormida, as well as from the main river. This result seems reasonable, because the minor is the distance from the outlet, the less are the reaches in which competition with other cascades reduce the transport capacity of the single cascade causing deposition and therefore potentially the interruption of the cascade. Moreover it is in accordance with results for the Da River presented by *Schmitt et al.* (2016) while using scenario 3 of competition, as well as with *Arnaud-Fassetta* (2004), who previously had observed on empirical data on the Rhone the decrease of the contribution of an upstream source to a downstream sink with the increasing distance between the two.

4.3 Grain size validation

The validation of the model outputs represents a challenge, because both grain size data and sediment fluxes data are difficult to collect. As for grain size mixture, the availability of observed data along two stretches of the Po River and the Stura di Demonte River allows a comparison with grain sizes simulated to be locally transported. Simulated data have been deprived of finer sediment fractions (i.e. $< 1\ cm$), which are not generally collected during field measurements.

Figures 4.3 and 4.4 show the comparison between simulated granulometric curves and measured grain size percentiles along rivers Po and Stura di Demonte respectively. Curves have been plotted for those reaches where observations come from.

While on one hand the simulation of median sediment mixtures for the Po River well replicates observed data, an underestimation of grain size emerges from the comparison of observed and simulated data related to the Stura di Demonte River. A certain underestimation seem to affect also coarser fractions of sediment collected in the Po River. This must be taken into account in the following because it could affect other validation results. Moreover the simulated grain size distributions seem to be quite close to each other, as in facts observations are much more scattered.

Both these kinds of mismatch with observed data may be due to the initialisation of grain size sources of cascades displayed in figure 4.1(a), herein derived by calculation under bankfull conditions (see 2.5) in absence of available data. In particular the loss in natural variability could derive from the choice of assigning just one source, and consequently one cascade and one grain size, per river reach. It is likely that initialising cascades with more accurate grain size data and assigning more than one cascade source carrying different grain sizes to each reach would lead to more diverse granulometric curves.

4.4 Sediment fluxes validation

Figure 4.5 allows another kind of basic validation based on sediment fluxes delivered to reaches through the comparison with previous estimates carried out by AdBPo (Autorità di Bacino del fiume Po) and Università degli studi di Bologna, which constitute the best data among the few available for the bed load fluxes in the Po.

Figure 4.5(a) shows how much sediment is delivered to every reach in terms of m^3/yr according to the results of the CASCADE simulation. In this case the concerned variables are the fluxes stored in MATLAB matrix `Input`, representing the sediment fluxes passing through reaches (expressed in kg/yr, so to be converted using sediment

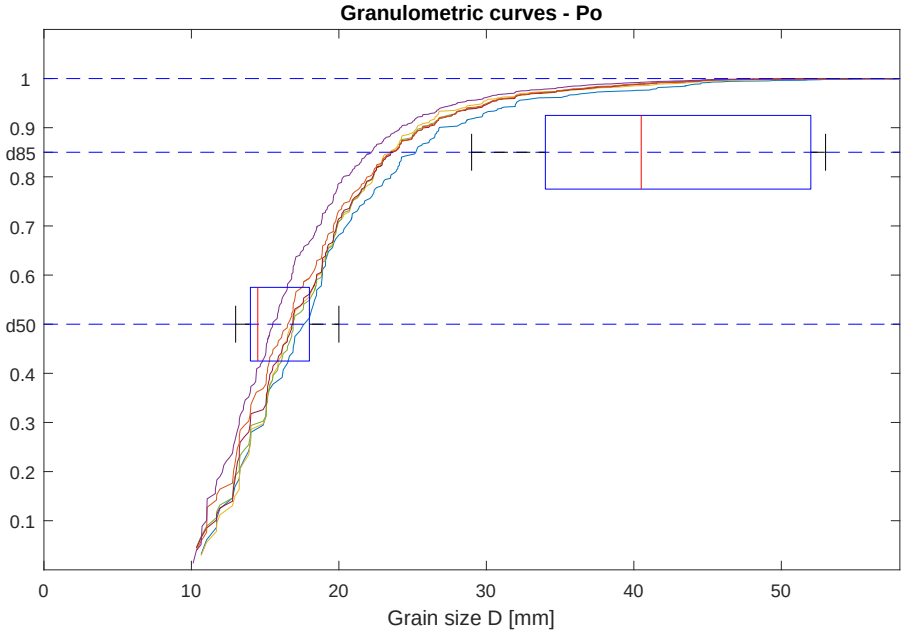

(a) Comparison between grain size field observations and simulated granulometric curves for the Po River: boxplots show the distribution of observed grain size percentiles d_{50} and d_{85} from samples collected in reaches highlighted in panel (b) (observed data from *PROGRAMMA GENERALE DI GESTIONE DEI SEDIMENTI ALLUVIONALI DELL'ALVEO DEL FIUME PO STRALCIO: CONFLUENZA STURA DI LANZO – CONFLUENZA TANARO, Relazione Tecnica*), *whereas simulated curves are referred to the same reaches.*

(b) Localisation of grain size measurements.

Figure 4.3: *Grain size validation for the Po River*

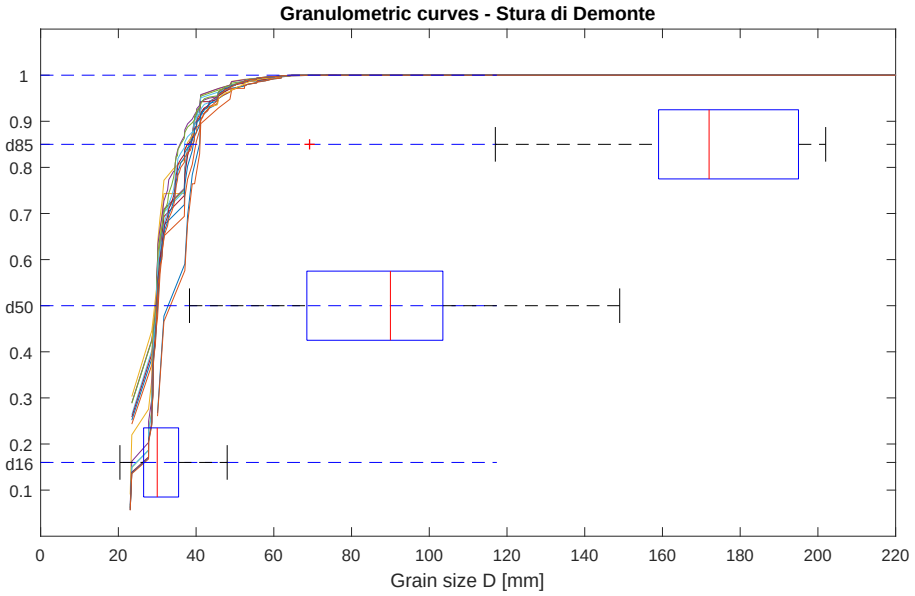

(a) Comparison between grain size field observations and simulated granulometric curves for the Stura di Demonte River: boxplots show the distribution of observed grain size percentiles d_{16}, d_{50} and d_{85} from samples collected in reaches highlighted in panel (b) (observed data from *Programma Generale di Gestione dei Sedimenti – Stralcio fiume Stura di Demonte, ANALISI DELLA COMPONENTE IDRAULICA*), *whereas simulated curves are referred to the same reaches.*

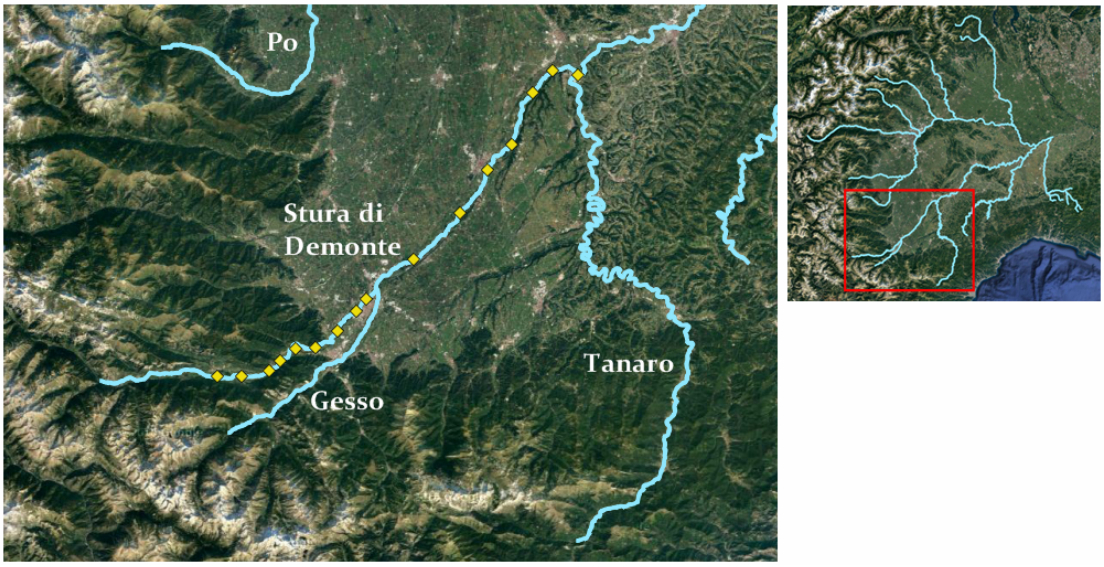

(b) Localisation of grain size measurements.

Figure 4.4: *Grain size validation for the Stura di Demonte River*

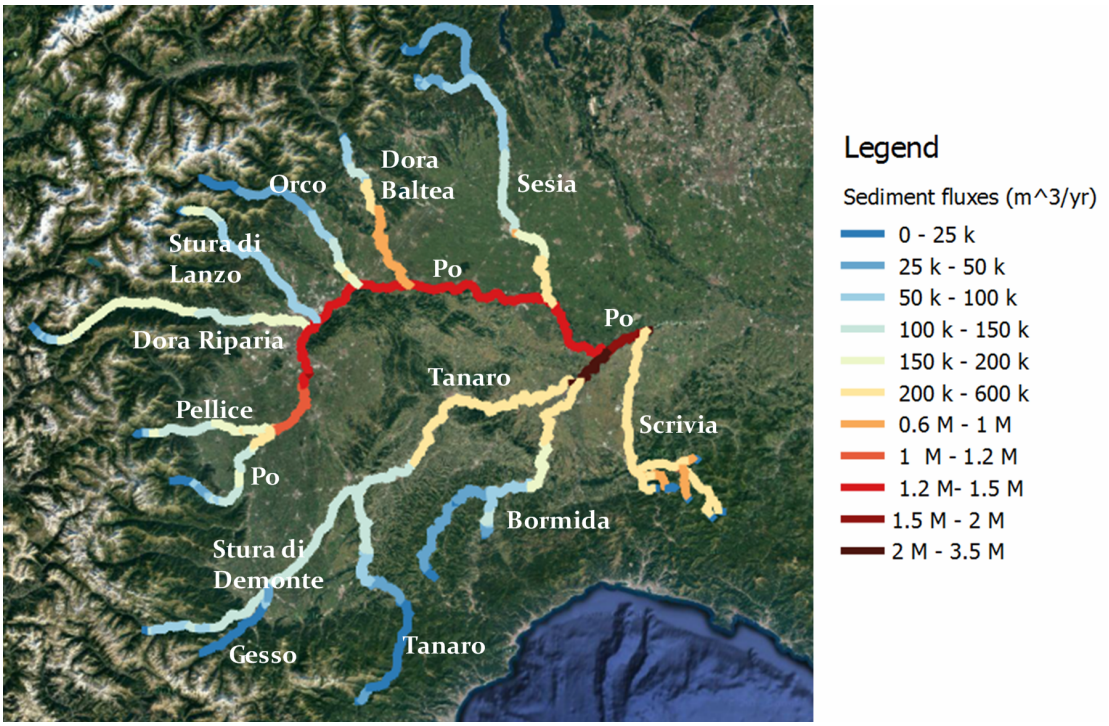

(a) Sediment fluxes $[m^3/yr]$ simulated by CASCADE over the Piedmont river network.

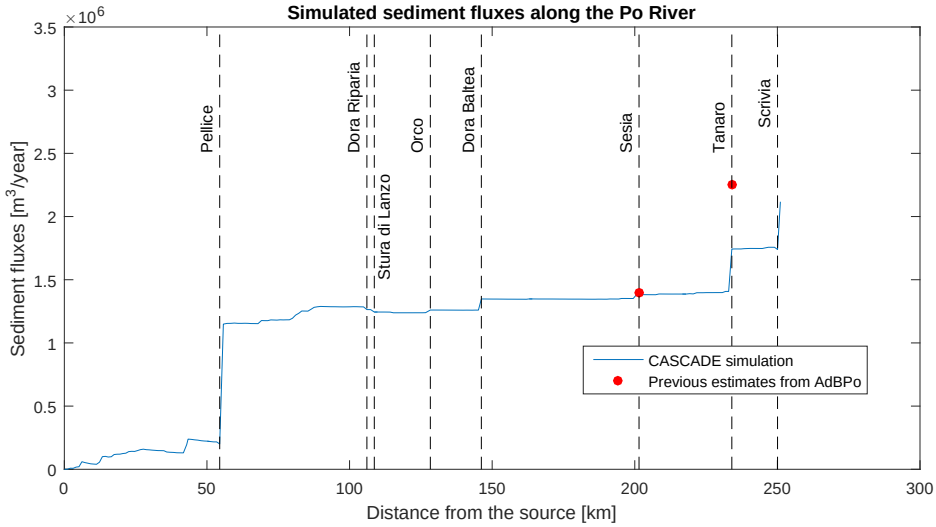

(b) Insight on CASCADE simulation of sediment fluxes $[m^3/yr]$ along the Po River and comparison with previous estimates from AdBPo (Autorità di bacino del fiume Po) in time 1982-2005.

Figure 4.5: *CASCADE simulations of sediment fluxes*

density $\rho_S = 2600\ kg/m^3$). The elements of the matrix are summed over columns in order to sum fluxes coming from every source ς and so obtaining total sediments fluxes delivered to every reach e. Resuming, sediment flux in every reach consists in the sum of fluxes of all the cascades passing through that reach.

Figure 4.5(b) shows an insight on fluxes simulated for the Po River (blue line) compared to local estimates of sediment fluxes in Mm^3/yr by AdBPo (red dots) at the con-

fluences with rivers Sesia and Tanaro, though referred to a different period (1982-2005) from the one taken for hydrological data used for CASCADE simulation (2004-2014). From results in these two sections of the Po River, it may be concluded that the model achieves to grasp at least the order of magnitude of fluxes. In detail at the confluence with Sesia both the CASCADE simulation and AdBPo estimate quantify fluxes about 1.3-1.4 Mm^3/yr, whereas a small underestimation seems to occur at the confluence with the Tanaro River, where sediment fluxes are around 2 Mm^3/yr).

Another confirmation of the right order of magnitude of simulated sediment fluxes arrives from estimates at Isola Serafini, about 100 km downstream of the network outlet. As reported by Spezzani, di Baldassarre and Montanari in *ARPA Rivista N. 4 luglio-agosto 2009*, studies of Università di Bologna have assessed sediment fluxes around 1.1 Mm^3/yr based on Engelund and Hansen formula, whereas other formulations have returned values between 1 and 2 Mm^3/yr.

Looking again at figure 4.5(a), within a general trend of progressive increase in downstream direction some decreases and sharp increases can be noticed, which might indicate a local tendency of the concerned river reach towards aggradation by deposition or instead incision by excessive detachment of sediments respectively. For instance a great increase of simulated sediment fluxes occurs along the last stretch of the Tanaro River: this means that CASCADE indicates erosion just more upstream of the confluence with the Bormida River, where input sediment fluxes are significantly lower than output fluxes. On the contrary reaches upstream of the confluence with the Po River may be subject to aggradation, since a decrease in sediment fluxes occurs before the Tanaro joins the Po. Figure 4.6 shows an insight on sediment fluxes simulated along the Tanaro river, displaying the profile discussed above. It would be interesting to verify if we are dealing with an incorrect estimation due to a problem of calibration of the model, or wrong initialisation as already discussed, or if such river stretches are actually at risk of bed incision. This could be linked to recent, and in part still present, problems of river bed incision and narrowing common for Central and Northern Italian rivers (*Surian and Rinaldi*, 2003).

4.5 Remarks

An overlook of presented results confirms the overall goodness of CASCADE performances. From the simulation of grain sizes and the delivery to the outlet a qualitative confirmation at the conceptual level of the simulation. Maps displaying simulated grain sizes produce a fining pattern from upstream to downstream both in the initialisation and in the median resulted from the routing. The simulation of fluxes instead provides a not only qualitative, but also quantitative validation of CASCADE performance, achieving to reproduce the order of magnitude of sediment fluxes. Better results, in particular as regards grain size simulation, could be achieved by providing a more accurate initialisation of sources grain size based on field measurements instead of estimates derived through hydraulic formulas. In addition simulating multiple sources of different grain sizes per reach could better reproduce natural variability in sediment distribution.

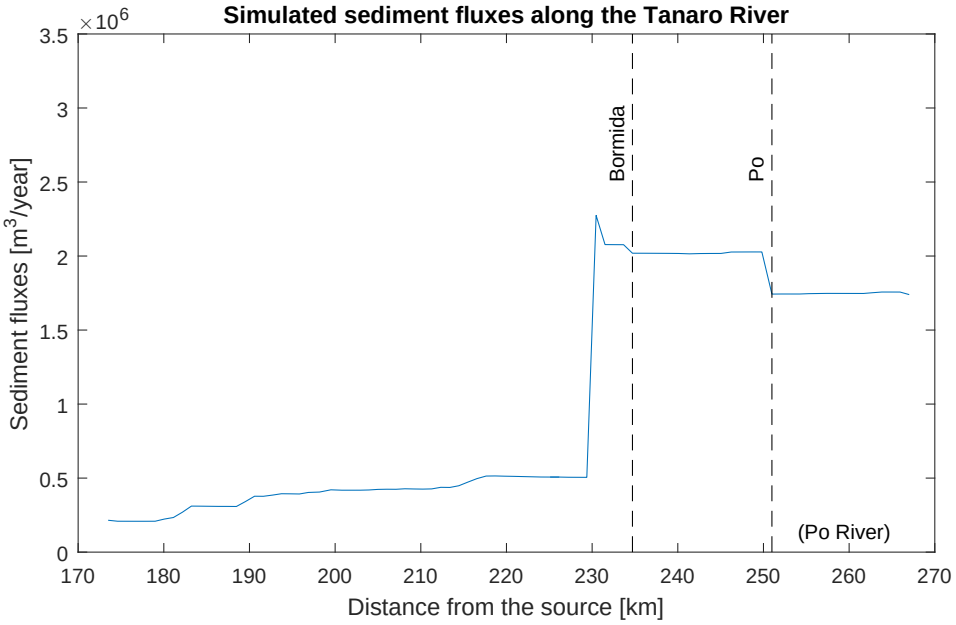

Figure 4.6: *Simulated sediment fluxes along the Tanaro River in its last stretch from Asti to the confluence into the Po River: the sharp increase just before the confluence with the Bormida River might indicate a tendency towards incision, whereas the decrease observed before the Po confluence might indicate aggradation.*

CHAPTER 5

Conclusions and future research

After presenting the CASCADE modelling framework both on a conceptual and on a detailed implementation plan, a practical application on the Upper Po river basin has been described. This represents a first validation of CASCADE model using spatially distributed sediment data, whereas previously applications concerned mainly poorly-monitored river basins. In terms of methodology, CASCADE was coupled in this thesis with a new module for extracting river network and topographic information from high-resolution LIDAR data.

The case study implementation allowed thus a validation of the model outputs, but also a practical understanding of the modelling framework and its implementation described in the first part of thesis, exploiting its potential. Specifically the versatility of CASCADE outputs, basically consisting of disaggregated information about transport of single sediment loads, allowed to simulate distributed quantities perfectly corresponding to locally available field observations (grain size) and other previous estimates (sediment fluxes), which made possible to carry out a basic validation of the model. The latter returned overall positive response; in detail best performances resulted along the Po River, as for median grain size estimates (around 15 mm), and at the Po-Sesia confluence, as for simulated sediment fluxes (around 1 million m^3/yr).

Besides verifying that quantitatively estimates were consistent with observed validation data, where no observations were available results were considered qualitatively reasonable (as for the fining trend from upstream to downstream in the map of median transported grain size, for instance).

Limitations and future development

During the case study application, several assumptions were made to carry out the simulation. Removing these limitations may represent a future direction to obtain better

results. One of these assumptions is represented by the analytical derivation of grain size initialisation. As evident from the grain distributions shown in the validation, initialisation based on hydraulic formulas under bankfull conditions may not return accurate estimates, but it is a reasonable alternative in absence of field measurements, which would provide a more appropriate initialisation. As an alternative, CASCADE has been applied also for inverse modelling in large river networks (*Schmitt et al.*, in review), concretely, to disaggregate single sediment observations into network-scale estimates of sediment flux and composition. Such an approach would be even more promising for the Upper Po basin, where multiple sediment observations are available throughout the river network.

Another improvement for the present work may be the introduction of multiple cascade sources per reach, in particular where minor tributaries or the upper stretch of rivers have not been included in the river network graph. Additional cascade sources in a reach could then reproduce sediment fluxes incoming from the same river upstream of that reach, in case of a source reach, or from neglected tributaries in case of a missed confluence reach. In both cases the additional cascade sources would generally transport a different grain size compared to that present in that reach. Moreover, if accurate local grain size information were available, multiple sources per each reach would allow to better describe the grain size composition of sediment fluxes originating in reaches.

In the case study herein presented the effect on connectivity of the several small reservoirs present throughout the Po river network was not simulated. Next step is then applying a newer version of CASCADE to implement the presence of dams, so that the model can be used to assess the negative impacts on sediment connectivity of such structures.

As regards the CASCADE modelling framework, this presents some approximations aimed to save computational efforts: it might be interesting to develop a more complex version of the model at the expense of calculation time, in order to see (maybe trying on case studies with relatively small basins, as for the Upper Po basin herein presented) if this results in more accurate outputs and what is the actual trade off with computational time. For instance, recursive iterations might lead to better estimates of transport capacities and grain sizes, or another improvement in this direction may be a more detailed description of reach sections: the assumption of rectangular shape is in fact good for channel-like rivers, but may be limiting in case of a more complex geometry.

Finally, as far as the Piedmont case study is concerned, it could be interesting to more thoroughly investigate on reaches indicated by mass balance of sediment fluxes to be at risk of river bed incision or aggradation, verifying if there is an actual correlation with observed alteration issues. In addition, CASCADE could be useful as a support tool for river and water management and for assessing the effectiveness at the network scale of sediment management measures (e.g. sediment reintroduction) meant to restore river morphology where subject to alteration issues.

Appendix

.1 Notation

A_D	Drainage Area $[km^2]$
C_f	Friction factor $[-]$
d	Grain size $[m]$
e	Specific edge (reach)
F	Competition Factor $[-]$
h	Water level $[m]$
I	Slope $[-]$
J	Hydrograph scaling factor
n_p	Number of observation within the $p-th$ discharge percentile $[-]$
n_{tot}	Total number of discharge observations for a reach $[-]$
p	Discharge percentile-defined class $[-]$
$\boldsymbol{Q}$	Discharge time series $[m^3\ s^{-1}]$
$Q_{1.5}$	1.5 year return period discharge $[m^3\ s^{-1}]$
Q_S	Transport capacity $[kg\ yr^{-1}]$
$Q_S{}'$	Competition corrected transport capacity $[kg\ yr^{-1}]$
$Q_{S,in}$	Sediment input $[kg\ yr^{-1}]$
q_{S*}	Dimensionless transport capacity $[-]$
q_S	Transport capacity per unit channel width $[m^2\ d^-1]$
R	Relative sediment density $[-]$
R_h	Hydraulic radius $[m]$
v	Flow velocity $[m\ s^{-1}]$
W_{AC}	Active channel width $[m]$
Γ	Set of sediment cascades
γ	Specific sediment cascade
Θ	Sediment flux $[kg\ yr^{-1}]$
κ	Cascade pathway
ρ_S	Sediment density $[kg\ m^{-3}]$
ς	Specific source

$\tau*$	Dimensionless shear stress $[-]$
τ_{*c}	Dimensionless critical shear stress $[-]$
ϕ_{thresh}	Percentage threshold to define cascade exhaustion $[-]$
Ω	Identifier of basin outlet node

.2 MATLAB coding

MATLAB function/script	CASCADE component	Description	Thesis section
calculateQsd50	Competition scenarios (within the cascade routing)	Script that calculates for every reach e the transport capacity $Q_{S_e}(d_{50_e})$ based on the median grain size d_{50_e} expected in that reach	Section 2.7
calculateQSin_s	Cascade routing	Function that returns the supply upper bounds and the bottle-neck reach for every cascade	Section 2.8
CalculateQsij_par_func	Derivation of transport capacities	Function that calculates the transport capacity $Q_{S_e^{\varsigma}}$ in every reach e for every cascade ς	Section 2.6
CASCADE_Func	Cascade routing	Main function of CASCADE model, it performs the calculation of corrected transport capacities $Q_{S_e^{\varsigma'}}$ and the routing of each cascade to simulate sediment fluxes Θ_e^{ς}	Section 2.8
createCascadeInputs	Cascade routing	Function used to group together all the inputs required for the cascade routing	Section 2.8
Engelund_Hansen	Derivation of transport capacities	Function that calculates the sediment transport according to the formulation proposed by Engelund and Hansen	Section 2.6
hydraulicCalc	Grain size solver	Function that derives an estimate of the local grain size d_{ς} in every source reach ς based on bankfull hydraulic conditions, providing the grain size initialisation of each cascade γ_{ς}	Section 2.5
HydraulicCalcs	Hydraulic calculations	Script that performs hydraulic calculations and the derivation of transport capacities $Q_{S_e^{\varsigma}}$	Section 2.6
hydraulicSolver	Hydrodynamic solver	Function that defines the objective function to be minimised through an iterating procedure, aimed to derive water level and flow velocity in a reach given a certain discharge	Section 2.5
Main_script_CASCADE _Piemonte	All the model's components	Script grouping all components required for the complete simulation	Chapter 2
slope_correction	Preprocessing	Function used to correct non-valid slopes due to any inaccuracies in raw elevation data	Section 2.4
parameterToMatrix	Grain size solver	Function that derives an origin-destination matrix from a vector whose elements are referred to the total set of cascades	Section 2.5
Wong_Parker	Derivation of transport capacities	Function that calculates the sediment transport according to the formulation proposed by Wong and Parker	Section 2.6

Table 1: *Cited MATLAB functions and scripts from CASCADE modelling framework*

MATLAB function/script	Description	Thesis section
ExtractRiverNetwork	Function that derives the graph for the river network and its attribute matrix from digital elevation data	Section 3.2.1
Main_script_CASCADE_Piemonte	Script grouping all components used for the complete simulation carried out for the Upper Po basin	Chapter 3
Script_adjust_drainage_area	Script used to correct drainage area in the attribute matrix of the river network	Section 3.2.2
Script_gauging_ stations	Script that associates gauging stations, in which observed hydrographs are available, to nodes of the river network.	Section 3.3.1
Script_merge_river_networks	Script used to merge two river networks having different level of detail	Section 3.2.1
Script_River_Network_Piemonte	Script used to set user-defined parameters for the extraction of the river network and to produce a shapefile of the graph with related attributes	Section 3.2.1
Script_wac	Script used to assign active channel width information to every reach of the river network based on areas of riverscape units	Section 3.2.3

Table 2: *Cited MATLAB functions and scripts specifically developed for the Upper Po basin implementation*

Bibliography

Andrews, E. D. (1983), Entrainment of gravel from naturally sorted riverbed material, *Geological Society of America Bulletin*, *94*(10), 1225–1231, doi: 10.1130/0016-7606(1983)94<1225:EOGFNS>2.0.CO;2.

Arnaud-Fassetta, G. (2004), The upper Rhône delta sedimentary record in the Arles-Piton core: Analysis of delta-plain subenvironments, avulsion frequency, aggradation rate and origin of sediment yield, *Geografiska Annaler: Series A, Physical Geography*, *86*(4), 367–383, doi: 10.1111/j.0435-3676.2004.00238.x.

ARPA PIEMONTE - Banca dati idrologica, url: `https://www.arpa.piemonte.gov.it/rischinaturali/accesso-ai-dati/annali_meteoidrologici/annali-meteo-idro/banca-dati-idrologica.html`

AUTORITÀ DI BACINO DEL FIUME PO (2007) - Programma generale di gestione dei sedimenti alluvionali dell'alveo del fiume Po, Stralcio: confluenza Stura di Lanzo - confluenza Tanaro.

AUTORITÀ DI BACINO DEL FIUME PO (2008) – Il recupero morfologico ed ambientale del fiume Po, Il contributo del Programma generale di gestione dei sedimenti del fiume Po.

Benda, L., and T. Dunne (1997), Stochastic forcing of sediment routing and storage in channel networks, *Water Resources Research*, *33*(12), 2865–2880, doi: 10.1029/97WR02387.

G. D. Betrie, Y. A. Mohamed, A. van Griensven and R. Srinivasan (2011), Sediment management modelling in the Blue Nile Basin, *Hydrol. Earth Syst. Sci.*, *15*, 807–818, doi: 10.5194/hess-15-807-2011.

Bizzi, S., and D. N. Lerner (2015), The Use of Stream Power as an Indicator of Channel Sensitivity to Erosion and Deposition Processes, *River Research and Applications*, *31*(1), 16–27, doi: 10.1002/rra.2717.

Bizzi, S., Schmitt, R. J. P., Giuliani, M., Castelletti, A. (2016), A modelling framework to evaluate human-induced alterations of network sediment connectivity and quantify their unplanned adverse impact. In Fall meeting of the American Geophysical Union: conference abstracts

Bracken, L. J., L. Turnbull, J. Wainwright, and P. Bogaart (2014), Sediment connectivity: a framework for understanding sediment transfer at multiple scales, *Earth Surface Processes and Landforms*, pp. n/a–n/a, doi: 10.1002/esp.3635.

Czuba, J. A., and E. Foufoula-Georgiou (2014), A network-based framework for identifying potential synchronizations and amplifications of sediment delivery in river basins, *Water Resources Research*, *50*(5), 3826–3851, doi: 10.1002/2013WR014227.

Czuba, J. A., and E. Foufoula-Georgiou (2015), Dynamic connectivity in a fluvial network for identifying hotspots of geomorphic change, *Water Resources Research*, *51*(3), 1401–1421, doi: 10.1002/2014WR016139.

Demarchi, L., S. Bizzi, and H. Piégay (2016), Hierarchical Object-Based Mapping of Riverscape Units and in-Stream Mesohabitats Using LiDAR and VHR Imagery, *Remote Sensing*, *8*(2), 97, doi: 10.3390/rs8020097.

Bibliography

Demarchi, L., S. Bizzi, and H. Piégay, Regional hydromorphological characterization with continuous and automated remote sensing analysis based on VHR imagery and low-resolution LiDAR data, accepted.

Engelund, F., and E. Hansen (1967), A monograph on sediment transport in alluvial streams, TEKNISKFORLAG Skelbrekgade 4 Copenhagen V, Denmark.

Jager, H. I., Efroymson, R. A., Opperman, J. J., Kelly, M. R. (2015), Spatial design principles for sustainable hydropower development in river basins, *Renewable and Sustainable Energy Reviews*, *45*, 808–816, doi: 10.1016/j.rser.2015.01.067.

Knighton, D. (1984), *Fluvial forms and processes*, E. Arnold, London; Baltimore, Md., U.I.A.

W. S. Merritt, R. A. Letcher, A. J. Jakeman (2003), A Review of Erosion and Sediment Transport Models, *Environmental Modelling and Software*, *18*(8–9), 761–799, doi: 10.1016/S1364-8152(03)00078-1.

Parker, C., C. R. Thorne, and N. J. Clifford (2015), Development of ST:REAM: a reach-based stream power balance approach for predicting alluvial river channel adjustment, *Earth Surface Processes and Landforms*, *40*(3), 403–413, doi: 10.1002/esp.3641.

Programma Generale di Gestione dei Sedimenti (2010) – Stralcio fiume Stura di Demonte.

Ranzi R., Le Hung T., Rulli M. C. (2012), A RUSLE approach to model suspended sediment load in the Lo river (Vietnam): Effects of reservoirs and land use changes, *Journal of Hydrology*: 422–423, 17–29, doi: 10.1016/j.jhydrol.2011.12.009.

Schmitt R. J. P. (2016), "CASCADE - A FRAMEWORK FOR MODELING FLUVIAL SEDIMENT CONNECTIVITY AND ITS APPLICATION FOR DESIGNING LOW IMPACT HYDROPOWER PORTFOLIOS", PhD Thesis at Politecnico di Milano Dipartimento di Elettronica, Informazione e Bioingegneria (DEIB).

Schmitt, R. J. P., Bizzi, S., Castelletti, A., (2015), Linking sediment connectivity to remotely sensed, reach-scale morphology identifies correlations between network-scale sediment regimes and local river processes and forms. In 2015 AGU Fall Meeting

Schmitt, R. J. P., Bizzi, S., Castelletti, A. (2015), Process based classification of sediment connectivity on the river basin scale, REFORM International Conference on River and Stream Restoration "Novel Approaches to Assess and Rehabilitate Modified Rivers", 30 June 2 July 2015, Wageningen. Conference proceedings pag.150–155

Schmitt, R. J. P., S. Bizzi, and A. F. Castelletti (2016), Tracking multiple sediment cascades at the river network scale identifies controls and emerging patterns of sediment connectivity, *Water Resources Research*, *52*, doi: 10.1002/2015WR018097.

Schmitt, R. J. P.; Bizzi, S.; Castelletti, A.; Rubin, Zan; Kondolf, G. Matthias (2016), Inverse modelling of fluvial sediment connectivity identifies characteristics and spatial distribution of sediment sources in a large river network. In Fall meeting of the American Geophysical Union: conference abstracts

Schmitt, R. J. P., S. Bizzi, and A. F. Castelletti and M. G. Kondolf, Inverse connectivity modeling for reconstructing sediment provenance and sediment fluxes in unmonitored river tributaries, in review.

Schwanghart, W. and Kuhn, N. J.(2010), TopoToolbox: A set of Matlab functions for topographic analysis, *Environmental Modelling & Software*, *25*,770–781, doi: 10.1016/j.envsoft.2009.12.002.

Schwanghart, W. and Scherler, D.(2014), Short Communication: TopoToolbox 2 – MATLAB-based software for topographic analysis and modeling in Earth surface sciences, *Earth Surface Dynamics*, *2*,1–7, doi: 10.5194/esurf-2-1-2014.

Soncini-Sessa, R., Castelletti, A., and Weber E., *Integrated and Participatory Water Resources Management - Theory*, Vol.1A, Elsevier Science, 2007

P. Spezzani, G.di Baldassarre, A. Montanari (2009), Idraulica del Po e scenari di trasporto solido allo stato attuale e in presenza di sbarramenti, *ARPA Rivista*, *4*, 16–17.

Surian N., Rinaldi M. (2003) Morphological response to river engineering and management in alluvial channels in Italy, *Geomorphology*, *50*,307–326, doi: 10.1016/S0169-555X(02)00219-2.

Wilcock, P. R., Crowe, J., 2003, Surface-based Transport Model for Mixed-Size Sediment, *Journal of Hydraulic Engineering*, *129*(2), 120–128, doi: 10.1061/(ASCE)0733-9429(2003)129:2(120).

Wilkinson, I. N., I. P. Prosser, and A. O. Hughes (2006), Predicting the distribution of bed material accumulation using river network sediment budgets, *Water Resources Research*, *42*(10), doi: 10.1029/2006WR004958.

Wolman, M. G., and J. P. Miller (1960), Magnitude and frequency of forces in geomorphic processes, *The Journal of Geology*, pp. 54–74.

Wong, M., and G. Parker (2006), Reanalysis and correction of bed-load relation of Meyer-Peter and Müller using their own database, *Journal of Hydraulic Engineering*, *132*(11), 1159–1168, doi: 10.1061/(ASCE) 0733-9429(2006)132:11(1159).